



1 **Responses of field-grown maize to different soil types, water regimes, and**
2 **contrasting vapor pressure deficit**

3 Thuy Huu Nguyen^{1,*}, Thomas Gaiser¹, Jan Vanderborght³, Andrea Schnepf³, Felix Bauer³, Anja
4 Klotzsche³, Lena Lärm³, Hubert Hüging¹, Frank Ewert^{1,2}

5 ¹University of Bonn, Institute of Crop Science and Resource Conservation (INRES), Katzenburgweg 5, 53115
6 Bonn, Germany

7 ²Leibniz Centre for Agricultural Landscape Research (ZALF), Institute of Landscape Systems Analysis,
8 Eberswalder Strasse 84, 15374 Muencheberg, Germany

9 ³Agrosphere (IBG-3), Institute of Bio- and Geosciences, Forschungszentrum Jülich GmbH, 52428, Jülich,
10 Germany

11 *Corresponding author, email: tngu@uni-bonn.de

12 **Abstracts**

13 Drought is a serious constraint to crop growth and production of important staple crops such as maize.
14 Improved understanding of the responses of crops to drought can be incorporated into cropping system
15 models to support crop breeding, varietal selection and management decisions for minimizing negative
16 impacts. We investigate the impacts of different soil types (stony and silty) and water regimes (irrigated
17 and rainfed) on hydraulic linkages between soil and plant, as well as root: shoot growth characteristics.
18 Our analysis is based on a comprehensive dataset measured along the soil-plant-atmosphere pathway at
19 field scale in two growing seasons (2017, 2018) with contrasting climatic conditions (low and high VPD).
20 Roots were observed mostly in the topsoil (10-20 cm) of the stony soil while more roots were found in the
21 subsoil (60-80 cm) of the silty soil. The difference in root length was pronounced at silking and harvest
22 between the soil types. Total root length was 2.5 - 6 times higher in the silty soil compared to the stony



23 soil with the same water treatment. At silking time, the ratios of root length to shoot biomass in the rainfed
24 plot of the silty soil (F2P2) were 3 times higher than those in the irrigated silty soil (F2P3) while the ratio
25 was similar for two water treatments in the stony soil. With the same water treatment, the ratios of root
26 length to shoot biomass of silty soil was higher than stony soil. The observed minimum leaf water potential
27 (ψ_{leaf}) varied from around -1.5 MPa in the rainfed plot in 2017 to around -2.5 MPa in the same plot of the
28 stony soil in 2018. In the rainfed plot, the minimum ψ_{leaf} in the stony soil was lower than in silty soil from
29 -2 to -1.5 MPa in 2017, respectively while these were from -2.5 to -2 MPa in 2018, respectively. Leaf water
30 potential, water potential gradients from soil to plant roots, plant hydraulic conductance ($K_{\text{soil_plant}}$),
31 stomatal conductance, transpiration, and photosynthesis were considerably modulated by the soil water
32 content and the conductivity of the rhizosphere. When the stony soil and silt soil are compared, the higher
33 'stress' due to the lower water availability in the stony soil resulted in less roots with a higher root tissue
34 conductance in the soil with more stress. When comparing the rainfed with the irrigated plot in the silty
35 soil, the higher stress in the rainfed soil resulted in more roots with a lower root tissue conductance in the
36 treatment with more stress. This illustrates that the 'response' to stress can be completely opposite
37 depending on conditions or treatments that lead to the differences in stress that are compared. To respond
38 to water deficit, maize had higher water uptake rate per unit root length and higher root segment
39 conductance in the stony soil than in the silty soil, while the crop reduced transpired water via reduced
40 aboveground plant size. Future improvements of soil-crop models in simulating gas exchange and crop
41 growth should further emphasize the role of soil textures on stomatal function, dynamic root growth, and
42 plant hydraulic system together with aboveground leaf area adjustments.

43 **Key words:** irrigation, plant hydraulic conductance, transpiration, root length, soil types, soil to leaf water
44 potential, stomatal regulation

45 **Abbreviations:** DOY: day of the year; DAS: day after sowing; TUE: transpiration use efficiency; SF: sap flow;
46 LAI: green leaf area index; PAR: photosynthetically active radiation; VPD: vapor pressure deficit; An: net



47 leaf photosynthesis; E : leaf transpiration; ψ_{leaf} : leaf water potential; $\psi_{\text{sunlitleaf}}$: leaf water potential of sunlit
48 leaf; $\psi_{\text{shadedleaf}}$: leaf water potential of shaded leaf; K_{soil} : hydraulic conductance of soil; K_{root} : root hydraulic
49 conductance; K_{stem} : stem hydraulic conductance; $\psi_{\text{soil_effec}}$: effective soil water potential; $\psi_{\text{difference}}$:
50 difference between effective soil water potential and sunlit leaf water potential; $K_{\text{soil_root}}$: root system
51 hydraulic conductance (includes soil and root hydraulic conductance); $K_{\text{soil_plant}}$: whole plant hydraulic
52 conductance (includes below and aboveground components).

53 **1. Introduction**

54 Maize (*Zea mays L.*) is a major staple crop throughout the world. Drought stress, which negatively affects
55 crop growth and yield, is of increasing concern in several important maize cultivating regions (Daryanto et
56 al., 2016). Increases in frequency and severity of drought events due to climate change have been recently
57 reported (IPCC, 2022). Thus, field observations and understanding on how maize responds to water stress
58 are necessary to suggest promising traits for breeding programs (Vadez et al., 2021) as well as irrigation
59 schemes (Fang and Su, 2019; Q. Cai et al., 2017). Improved understanding of crops' response to drought
60 can be incorporated into soil-crop models (e.g. crop modelling and soil-vegetation-atmosphere transfer
61 modelling).

62 Stomatal regulation is often considered as a key aboveground hydraulic variable in regulating water use
63 of crops. Maize was considered as isohydric plant in which stomata are closed in response to sensing
64 drought conditions to maintain leaf water potential (ψ_{leaf}) above critical levels ($\psi_{\text{threshold}}$ or minimum ψ_{leaf})
65 (Tardieu and Simonneau, 1998). Investigations of how stomatal controls differ among species and
66 genotypes commonly observed minimum ψ_{leaf} or analyzed of genetic variability of stomatal control in
67 response to varying soil water content. Analyzing measurements of ψ_{leaf} from 400 lines of maize of tropical
68 and European origins under greenhouse and growth chamber conditions, Welcker et al. (2011) reported
69 values of minimum ψ_{leaf} from -0.8 to -1.5 MPa, indicating genetic variability of stomatal responses. The
70 isohydric behavior is due to different mechanisms including hydraulic and/or chemical (e.g. abscisic acid



71 [ABA]) signals (Tardieu, 2016). The degree to which these underlying mechanisms interact and differ
72 among genotypes and/or environmental scenarios in explaining the stomatal regulation is still debated
73 (Tardieu, 2016, Hochberg et al., 2018). Field evidence in variation of the minimum ψ_{leaf} of maize due to soil
74 water availability is rarely reported.

75 Water flow along the soil-plant-atmosphere continuum is determined by a series of hydraulic
76 conductivities and gradients in water potential. Hydraulic conductance of soil (K_{soil}), root hydraulic
77 conductance (K_{root}), and stem hydraulic conductance (K_{stem}) determine water potential from soil to root
78 and root xylem water, and thus magnitude of ψ_{leaf} . There are two main resistances to water flow from the
79 soil to the shoot, namely the soil and the root resistances, often expressed as their inverse, K_{soil} and K_{root}
80 (Nguyen et al., 2020; Cai et al., 2018). In wet soils, the soil hydraulic conductivity is much higher than that
81 of roots, and water flow is mainly controlled by root hydraulic conductivity (Hopmans and Bristow, 2002;
82 Draye et al., 2010). It is well-known that a decrease in soil matric potential and soil hydraulic conductivity
83 triggers stomatal closure and thus results in reduction in transpiration rate (Sinclair and Ludlow, 1986;
84 Carminati and Javaux 2020; Abdalla et al., 2021). For the root water uptake and controlling stomata, the
85 location where soil and roots are in close contact (rhizosphere) is most important, because when this thin
86 layer of rhizosphere is disconnected (i.e. soil-root contact is lost), the water movement from soil toward
87 the roots is reduced, which might trigger stomatal closure to maintain hydraulic integrity of plant
88 (Carminati et al., 2016; Rodriguez-Dominguez and Brodribb, 2019; Abdalla et al., 2022). The magnitude of
89 the drop of water potential between bulk soil and soil-root interface increases considerably at different
90 levels of soil dryness for different soil types (Carminati and Javaux, 2020; Abdalla et al., 2022). Hydraulic
91 limits in the soil (Carminati and Javaux, 2020), or in the root–soil interface [as measured for olive trees by
92 Rodriguez-Dominguez and Brodribb, 2019 or tomato (Abdalla et al., 2022)], or in the root properties
93 (Bourbia et al., 2021; Cai et al., 2022; Nguyen et al., 2020; Cai et al., 2018) or due to both soil textures and
94 root phenotypes (Cai et al., 2022b) emphasized the importance of belowground hydraulics (Carminati and



95 Javaux, 2020). However, also the shoot hydraulic conductance could be limiting in some crop plants
96 (Gallardo et al., 1996) or in trees (Domec and Pruyn, 2008; Tsuda and Tyree, 1997). Stomatal conductance
97 and shoot hydraulic conductance showed close links to each other in pine trees (Hubbard et al., 2001).
98 This summary illustrates three points: (i) current studies have often focused either on above or on below
99 hydraulic limits, but rarely consider both (ii) it is unclear the roles and relations of soil hydraulic properties
100 to root and plant hydraulic conductance (thus influences on stomatal conductance) (iii) the role of different
101 hydraulic processes across the soil - plant - atmosphere continuum i.e. soil to roots, stem, and soil-plant
102 hydraulic conductance in controlling stomatal conductance remains unclear.

103 Simultaneous measurements of atmospheric conditions (light intensity and vapor pressure deficit), leaf
104 water potential, and transpiration rates, coupled with measurements of root, stem and whole soil-plant
105 hydraulic conductance, root architecture, and soil water potential distribution could reveal the relative
106 importance of rhizosphere, shoot and root growth, and hydraulic conductance vulnerability, especially
107 under progressive soil drying at field conditions (Carminati and Javaux, 2020; Tardieu et al., 2017). For the
108 soil water conditions, soil texture and hydraulic characteristics are very important that influence soil water
109 movement and thus affect infiltration, surface and sub-surface runoff, and ultimately plant available soil
110 water (Vereecken et al., 2016). Soil texture properties, characterized by different fractions of clay, silt, and
111 sand particles, are important drivers in determining the soil water retention properties (Scharwies and
112 Dinneny, 2019; Stadler et al., 2015; Zhuang et al., 2001). Soil with higher water holding capacity (here the
113 silty soil with low stone content) have a larger amount of plant available water which in turn enables crops
114 to better meet the evaporative demand and facilitates better crop growth as compared to the soil with
115 high stone content (Nguyen et al., 2020; Cai et al., 2018). Estimations of hydraulic conductance (different
116 organs and whole plant hydraulic conductance) were done for crop plants and maize mainly under
117 controlled environment or pot conditions e.g. for different species and genotypes during soil drying (Sunita
118 et al., 2014; Choudhary and Sinclair, 2014; Abdalla et al., 2022; Meunier et al., 2018; Wang et al., 2017; Li



119 et al., 2016) or various species and genotypes together with different soil textures (Cai et al., 2022a), or
120 soil texture with different vapor pressure deficit (VPD) (Cai et al., 2022b). Compared to the substantial
121 effect of soil texture, there was no evidence of an effect of VPD on both soil–plant hydraulic conductance
122 and on the relation between canopy stomatal conductance and soil–plant hydraulic conductance in pot-
123 grown maize (Cai et al., 2022b). Contrast results were found in winter wheat where plant hydraulic
124 conductance increased with rising VPD for some genotypes in wet conditions (Ranawana et al., 2021).
125 Vadez et al., (2021) examined the effects of soil types together with increasing VPD on transpiration
126 efficiency (TE) and yield under pot conditions for several C₄ species (maize, sorghum, and millet). The
127 interpretation of differences in TE was attributed to soil types, more specifically, to the differences in soil
128 hydraulic properties and soil hydraulic conductance. However, experimental evidence linking root
129 hydraulics to stomatal regulation was lacking in these two Vadez’s studies (Vadez et al., 2021).
130 Extrapolation and use of results obtained in pots or under greenhouse conditions to the field scale are
131 difficult due to the fact that soil substrates in pots might not represent natural soil in the field (Passioura,
132 2006). There is often greater evaporative demand and considerable fluctuation and interactions of climatic
133 variables in the field as compared to experiments under controlled or semi-controlled conditions. Recent
134 field studies have aimed at quantification of root hydraulic conductance and its linkages with crop growth
135 (leaf area and biomass) under different soil types (in wheat Cai et al., 2017; Cai et al., 2018; Nguyen et al.,
136 2020 or maize in Nguyen et al., 2022; Jorda et al., 2022). However, field studies that consider both below
137 (soil–root hydraulic conductance) and above (stem hydraulic conductance), or soil–plant hydraulic
138 conductance (includes below and above-ground parts) and their roles in stomatal regulation as well as
139 crop growth (leaf area and biomass) are rarely carried out.

140 This study aims at further understanding of the hydraulic linkages between soil and plant and responses
141 of plants to drought stress in relation to root: shoot growth characteristics at field scale. We hypothesize
142 that, in field-grown maize, (1) soil–plant hydraulic conductance depends on soil hydraulic properties,



143 especially under dry soil conditions (2) minimum leaf water potential of maize is similar across soil types,
144 water treatments and climatic conditions. The hypotheses will be tested through three objectives: (i) to
145 investigate the effects of soil types, water application, and climatic condition on root growth and (ii) on
146 stomatal conductance, leaf photosynthesis, transpiration, leaf water potential, different components
147 (root, stem and whole soil-plant hydraulic conductance), and (iii) to analyze the relative contribution of
148 root and shoot growth (leaf area and biomass) on the water uptake capacity of maize. These three
149 objectives will be achieved based on a comprehensive dataset covering the whole soil-plant continuum
150 over two growing maize seasons with contrasting climatic conditions (low and high VPD) under two water
151 treatments (rainfed and irrigated) and two different soil types (stony and silty soil).

152 **2. Materials and methods**

153 **2.1. Location and experimental set-up**

154 We carried out a field experiment at two rhizotron facilities in Selhausen, North Rhine-Westphalia,
155 Germany (50°52'N, 6°27'E). The field is slightly inclined with a maximum slope of around 4°. One rhizotrone
156 facility was located upslope (F1) with around 60% gravel by weight in the 10-cm topsoil while the second
157 rhizotrone facility was at downslope (F2) with silty soil (stone content is around 4% by weight).

158 Each experimental site was divided into three subplots of 7.25 m by 3.25 m: two rainfed plots (P1, P2), and
159 one irrigated plot (P3). In rainfed plots P1, other sowing densities and dates were used than in the other
160 plots and we excluded therefore these plots. Silage maize cv. Zoey was sown on 4 May and 8 May in 2017
161 and 2018, respectively, with a plant density of 10.66 seeds m⁻² (Figure 1a; Table 1). Detailed information
162 of crop management practices is provided in Table 1.

163 [Insert Table 1 here]



164 **2.2. Water applications**

165 Weather variables (global radiation, temperature, relative humidity, precipitation, and wind speed) were
166 recorded every 10 minutes by a nearby weather station (approx. 100 m from the experiment). Drip lines
167 (T-Tape 520-20-500, Wurzelwasser GbR, Müzenberg, Germany) were installed for irrigation at 0.3 m
168 intervals parallel to the crop rows. In 2017, maize received a total amount of 230 mm precipitation during
169 the growing period (136 days). Average, minimum and maximum daily air temperature were 17.6, 8.3, and
170 25.3 °C, respectively (Fig. 1b). The crop on P3 was irrigated (in total 130 mm) every 5-7 days (in total 10
171 times) using 13 mm of irrigation water per event between mid June to end of August for the irrigated plots
172 (2017F1P3 and 2017F2P3) (Fig. 1b). In 2018, average, minimum, and maximum daily air temperature were
173 19.2, 10.85, and 27.3 °C, respectively (Fig. 1b) and exceeded those of 2017. Characterized by exceptionally
174 hot and dry weather conditions, the summer season 2018 can be classified as an extreme year with respect
175 to plant growth at our site. Maize experienced high temperatures and VPD, especially around tasseling
176 and silking. In 2018, only 91.3 mm of rain were recorded in the growing period of 2018 (107 days). The
177 maize crop was irrigated every 5-7 days (in total 13 times), with a total amount of irrigation of 257 mm
178 and 239 mm between mid- June and mid- August for the irrigated plots 2018F1P3 and 2018F1P3,
179 respectively (Fig. 1d). In contrast to 2017, the rainfed plot in the stony soil (2018F1P2) had to be irrigated
180 (in total 66 mm) in four times (using 13, 22, 13, and 18 mm, respectively) to avoid a crop failure due to
181 severe drought (Fig. 1d).

182 [Insert Figure 1 here]

183 **2.3. Measurements**

184 **2.3.1. Soil water measurement and root growth**

185 At soil depths of 10, 20, 40, 60, 80, and 120 cm, MPS-2 matrix water potential and temperature sensors
186 (Decagon Devices Inc., UMS GmbH München, Germany) were installed to measure half-hourly soil water
187 potential and soil temperature. The range of the water potential measurements is from -9 kPa to



188 approximately -100000 kPa (pF 1.96 to pF 6.01). In addition to MPS-2, soil water potential was measured
189 by pressure transducer tensiometers (T4e, UMS GmbH, München, Germany) where the minimum
190 detectable suction is -85 kPa to +100 kPa. A detailed description of sensor installation, calibration and data
191 post processing can be found in Cai et al., (2016).

192 Minirhizotubes (7 m long clear acrylic glass tubes with outer and inner diameters of 6.4 and 5.6 cm,
193 respectively) were installed horizontally at six different depths of 10, 20, 40, 60, 80, and 120 cm below the
194 soil surface in each facility. There are three replicate tubes at each depth, accounting for 54 tubes in each
195 facility. Root measurements were taken manually by Bartz camera (Bartz Technology Corporation) (23
196 June 2017 – 12 September 2017) and VSI camera (Vienna Scientific Instruments GmbH) (08 June 2017 – 22
197 June 2017) in 2017 while only VSI was used in 2018 (23 May 2018 - 23 August 2018). Root images were
198 repeatedly taken from both left and right sides at 20 locations along horizontally installed minirhizotubes.
199 The root images were analyzed by automated minirhizotube image analysis pipeline for segmentation and
200 automated feature extraction (Bauer et al., 2021). Two-dimensional root length density (RLD, in units of
201 cm cm^{-2}) was estimated from the total root length observed in the image and the image surface area. The
202 overview of camera system, minirhizotube images acquisition, and post-processing of the root data were
203 described in detail in Bauer et al. (2021).

204 **2.3.2. Crop growth measurement**

205 The phenology, plant height, stem diameter, green and brown leaf area, dry matter of different organs,
206 and total aboveground dry matter were observed and measured bi-weekly. Plant height was measured of
207 15 randomly selected plants. The diameters of five randomly selected stems were measured. Due to the
208 limited number of plants in each plot, only two plants per measurement date were sampled to determine
209 total aboveground dry matter and leaf area (7 and 8 times in 2017 and 2018, respectively). Green and
210 brown leaf area was measured by a LI-3100C (Licor Biosciences, Lincoln, Nebraska, USA). At harvest, five



211 separate replicates (1m² each) were harvested. The dry matter of separate organs was determined after
212 drying at 105 °C for 48 hours (Nguyen et al., 2020).

213 **2.3.3. Leaf gas exchange, leaf water potential, and sap flow measurements**

214 Hourly leaf stomatal conductance (Gs), net photosynthesis (An), and leaf transpiration (E) were measured
215 every two weeks under clear sky conditions. Observations from 8 AM to 5 PM on four days and from 10
216 AM to 4 PM on six days were carried out in 2017. In 2018, measurements were carried out on 6 days from
217 8 AM to 7 PM and on 5 days from 10 AM to 4 PM (Nguyen et al., 2022a). The Gs, An, and E of two sunlit
218 leaves (uppermost fully developed leaves) and one shaded leaf of different plants were measured at
219 steady-state using a LICOR 6400 XT device (Licor Biosciences, Lincoln, Nebraska, USA). After leaf gas
220 exchange measurements, leaves were quickly detached using a sharp knife to measure leaf water potential
221 (ψ_{leaf}) with a digital pressure chamber (SKPM 140/ (40-50-80), Skye Instrument Ltd, UK) with the working
222 air pressure ranging from 0 to 35 bars. To study the diurnal course of ψ_{leaf} under dry and re-wetted soil
223 conditions, in 2018, measurements were undertaken for three additional days with predawn
224 measurements two days before and one day after irrigation. Further detail of measurement dates, range
225 of real time records of PAR, VPD and soil water status could be found in (Nguyen et al., 2022a).

226 In 2017 (from 7 July 2017 until harvest) and 2018 (from 28 June 2018 until harvest), 20 sap flow sensors
227 (SGA 13, SGB 16, and SGB 19 types) were installed (one sensor per plant and 5 maize plants per plot) based
228 on stem diameter size. Sensor data, in particular the partitioning of energy, electricity supply, sap flow,
229 and the temperature difference between upper and lower thermocouples (dT) of each sensor were
230 recorded at 10 minute intervals using a CR1000 data logger and two AM 16/32 multiplexers (Campbell
231 Scientific, Logan, Utah). The sap flow in the plant (g h⁻¹) was monitored directly by the data loggers
232 (Dynamax, 2007) and used as a surrogate for canopy transpiration based on the number of plants per
233 square meter.



234 **2.4. Calculation of total root length, root system conductance, stem, and whole plant hydraulic**
235 **conductance**

236 To estimate the total root length from minirhizotubes, we adopted the option 2 which was described in
237 Cai et al., (2017). Total root length per square meter soil surface area within each soil layer ($m\ m^{-2}$) was
238 computed by multiplying the root length density with the corresponding soil layer thickness. The root
239 length density was determined in each depth by dividing the measured root length per minirhizotron
240 image by the assumed volume the roots would have occupied in absence of the tube, i.e., $W * L * \text{tube}$
241 radius (see Cai et al., 2017).

242 Following Nguyen et al., (2020), the effective soil water potential was calculated based on hourly measured
243 soil water potential (ψ_i) and normalized root length density at six depths (10, 20, 40, 60, 80, and 120 cm)
244 (NRLD_i), and soil layer thickness (Δz_i) in the soil profile (Equation 1).

$$\psi_{soil_effec} = \sum_{i=1}^N \psi_i NRLD_i \Delta z_i \quad (1)$$

245 We followed Ohm's law analogy by dividing the hourly sap flow by the difference between effective soil
246 water potential and shaded leaf water potential to estimate root system conductance (K_{soil_root} - Equation
247 2), between shaded leaf water potential and sunlit leaf water potential to estimate stem hydraulic
248 conductance (K_{stem} - Equation 3), and between effective soil water potential and sunlit leaf water potential
249 to estimate whole plant hydraulic conductance (K_{soil_plant} - Equation 4).

$$K_{soil_root} = Sapflow / (\psi_{soil_effec} - \psi_{shadedleaf}) \quad (2)$$

$$K_{stem} = Sapflow / (\psi_{shadedleaf} - \psi_{sunlitleaf}) \quad (3)$$

$$K_{soil_plant} = Sapflow / (\psi_{soil_effec} - \psi_{sunlitleaf}) \quad (4)$$



250 During one measurement day, four values of the $K_{\text{soil_root}}$, K_{stem} , and $K_{\text{soil_plant}}$ were obtained from
251 measurements between 11AM and 2 PM. The average and standard deviation of these hourly
252 measurements were calculated for each measurement day in order to present the seasonal dynamics of
253 those variables. To capture the diurnal and seasonal variations of sap flow and sunlit leaf water potential,
254 in addition, we plotted the hourly sap flow and hourly difference of effective soil water potential and sunlit
255 leaf water potential for three measurement days starting from predawn and whole seasons, respectively,
256 to derive the slope which is also $K_{\text{soil_plant}}$.

257 **2.5. Statistical analysis**

258

259 Regression analysis was performed to understand the relationship between the sap flow volume and the
260 difference of effective soil water potential and sunlit leaf water potential as well as the relationship
261 between the total aboveground biomass and cumulated water transpired (sap flow volume). These
262 analyses allow to derive the slope as proxy of $K_{\text{soil_plant}}$ and transpiration use efficiency, respectively. Since
263 all measured data have their own measurement errors, the generalized Deming regression was employed.
264 We performed relationships (via correlation coefficient and statistical significant levels) of midday leaf A_n ,
265 G_s , and E with midday K_{stem} , $K_{\text{soil_plant}}$, $K_{\text{soil_root}}$, sunlit leaf potential, $\psi_{\text{soil_effec}}$, and the difference of $\psi_{\text{soil_effec}}$
266 and sunlit leaf water potential ($\psi_{\text{difference}}$). All data processing and analysis were conducted using the R
267 statistical software (R Core Team, 2022).

268 **3. Results**

269 **3.1. Root growth under different water treatments, soil types and climatic conditions**

270 Observed root length (cm cm^{-2}) from the minirhizotubes in different soil depths at the first week of June
271 (stem elongation), around silking, and at harvest in two growing seasons are shown in the Figure 2. Root
272 length was similar among water treatments at the start of stem elongation in both years (Fig. 2a & 2d).
273 The difference in root length was pronounced at silking and harvest between the soil types. More root
274 growth was observed in the silty soil compared to the stony soil with the same water treatment (i.e. 2.5 -



275 6 times higher at depth 40 cm). This indicated the strong negative effects of stone content on root
276 development. In the stony soil, root length in the irrigated plot (F1P3) was slightly higher than in the rainfed
277 plot (F1P2). In contrast, the rainfed treatment (F2P2) in the silty soil showed much higher root length,
278 especially from 40 to 120 cm depths as compared to the irrigated plot (F2P3) in both growing seasons.
279 Much lower stone content and deep soil cracks in the silty soil (Morandage et al., 2021) allow root
280 extension to the subsoil, particularly in the rainfed plot F2P2. Root length in the rainfed treatment (F2P2)
281 in 2018, is higher than in 2017 which implies that root further developed to exploit the water in the soil
282 under the rainfed condition to meet the higher evaporative demand.

283 [Insert Figure 2 here]

284 Total root length (m m^{-2}) estimated from minirhizotubes and its ratio to shoot dry matter (m kg^{-1}) at three
285 measured dates (as in Figure 2) are shown in the Figure 3. Total root length was much higher for the silty
286 plots as compared to stony plots. In 2017, the highest total root length was observed in the rainfed plot of
287 the silty soil (F2P2) with approximately 9166 m m^{-2} and 9878 m m^{-2} around silking and harvest, respectively,
288 which was almost two times higher than in the irrigated plot (F2P3). These figures were higher in 2018
289 than 2017 where total root length of F2P2 was 10188 m m^{-2} and 13750 m m^{-2} at silking and harvest time,
290 respectively. For the rainfed stony soil (F1P2), soil water depletion around the beginning of June in 2017
291 (Supplementary material 1a) and from the first two weeks of June to harvest in 2018 (Supplementary
292 material 2a) caused the strong reduction of shoot biomass. In the stony soil, the shoot dry matter of the
293 irrigated plot (F1P3) and the rainfed plot (F1P2) were 1275 and 536 g m^{-2} at silking time (e.g. 19 July 2018
294 –DOY 200, Supplementary material 3a and 3b). However, there was a minor difference between F1P2 and
295 F1P3 in terms of the ratio of root length to shoot dry matter. In the silty soil, a decrease of soil water
296 potential was not pronounced (compared to stony soil) in both years 2017 and 2018 (Supplementary
297 material 1b and 2b). In 2018, shoot biomass in the irrigated stony soil (F1P3) and silt soil (F2P3) were
298 similar (1275 and 1299 g m^{-2} , respectively on 19 July 2018 – DOY 200) while the shoot biomass of the



299 rainfed silty soil (F2P2) was 876 g m^{-2} (Supplementary material 3a & 3b). However, the ratios of root length
300 to shoot biomass in the rainfed plot of the silty soil (F2P2) were 3 and 6 times higher than those in the
301 irrigated silty soil (F2P3) and stony soil (F1P3), respectively (e.g. 18 July, DOY 199). Moreover, total root
302 length was relatively equal among treatments at the start of set elongation (DOY 159, first week of June)
303 in both years, while this was the opposite for the ratio of root length to shoot dry matter. This firstly
304 illustrated that the finer soil texture without stones and with soil cracks could favor the root growth which
305 indicates strong interactions of root and soil conditions. Secondly, the larger root length and higher
306 atmospheric evaporative demand in 2018 than 2017 indicates also the interaction of root growth and
307 climatic conditions.

308 [Insert Figure 3 here]

309 **3.2. Stomatal conductance, photosynthesis, transpiration, and $K_{\text{soil_plant}}$**

310 **3.2.1. Diurnal course of stomatal conductance, photosynthesis, transpiration, and water potential at leaf** 311 **level**

312 After a long period with high temperatures and no rainfall, soil water reduction in the rainfed plot of the
313 stony soil (F1P2) on 17 July 2018 (Supplementary material 2) resulted in three times lower net
314 photosynthesis (A_n), stomatal conductance (G_s), transpiration (E) and leaf water potential (ψ_{leaf}) as
315 compared to the remaining treatments (Fig. 4). This indicates that the soil water content strongly affected
316 the stomatal conductance. Stomatal closure was much pronounced around midday in F1P2 while this was
317 not the case in the F2P2, indicating the soil type strongly affected the stomatal conductance and leaf gas
318 exchange.

319 [Insert Figure 4 here]

320 Leaf gas exchange and leaf water potential in the F1P2 were still much lower than in other plots (Figure
321 5). On 18 July 2018, after application of 22.75 mm of irrigation water (at 4 PM), photosynthesis, stomatal



322 conductance, transpiration and leaf water potential were slightly increased in F1P2. However, these were
323 still smaller than in F2P2 and the two irrigated plots.

324 [Insert Figure 5 here]

325 On the next day after irrigation, leaf gas exchange and water potential were considerably increased in the
326 F1P2 (Figure 6). Leaf curling was also less pronounced as compared the two previous days. This indicated
327 the recovery of plant after watering. Leaf water potential, photosynthesis, stomatal conductance, and leaf
328 transpiration were almost similar to other plots from predawn throughout the day.

329 [Insert Figure 6 here]

330 **3.2.2. Seasonal course of stomatal conductance, photosynthesis, transpiration, water potential, and** 331 **plant hydraulic conductance at the leaf level**

332 Seasonal stomatal conductance (G_s) and leaf water potential (ψ_{leaf}) are described in Figure 7. The
333 relationship between two variables was rather noisy and non-linear. The leaf water potential showed
334 distinct patterns among treatments in one growing season. Minimum ψ_{leaf} was maintained at around -1.5
335 MPa in the irrigated plot in stony soil (F1P3) and two plots in the silty soil (F2P2 and F2P3). Lower minimum
336 ψ_{leaf} could be observed in the rainfed plot with stony soil (F1P2) but it did not go beyond -2 MPa. Minor
337 leaf curling was observed only in the second week of June in the F1P2 in 2017. In 2018, the higher
338 temperature and vapor pressure deficit resulted in lower minimum ψ_{leaf} in all treatments and soil types as
339 compared to 2017. The minimum ψ_{leaf} was around -2 MPa in F1P3, F2P2, and F2P3 while ψ_{leaf} could drop
340 below -2 MPa in F1P2 which was due to the severe soil water deficit. The low G_s and ψ_{leaf} associated with
341 measurement dates when the substantial leaf curling was observed at mid of July to the end of growing
342 season in F1P2 in 2018 (Supplementary material 3c & 3d and Supplementary material 4c & d).

343 [Insert Figure 7 here]



344 The effective soil water potential ($\psi_{\text{soil_effect MD}}$), sunlit leaf water potential ($\psi_{\text{sunlitleaf MD}}$), stomatal
345 conductance (G_{SMD}), and whole plant hydraulic conductance ($K_{\text{soil_plant MD}}$) at midday at several times during
346 the growing season are presented in Figures 8 and 9 for 2017 and 2018, respectively. As expected, there
347 was not much difference in terms of $\psi_{\text{soil_effect MD}}$ among F1P3, F2P2, and F2P3 from 02 August to one week
348 before harvest in 2017. The lowest $\psi_{\text{soil_effect MD}}$ was observed in the F1P2. Leaf water potential dropped
349 drastically but also $K_{\text{soil_plant MD}}$ increased strongly whereas $\psi_{\text{soil_effect MD}}$ remained quite similar (e.g. 18 July).
350 This is because sap flow have increased substantially in this day (e.g. from 2.34 mm d⁻¹ on 17 July to 6.97
351 mm d⁻¹ on 18 July for the F1P2). The stomatal conductance decreased a lot in this day which could be
352 explained that the atmospheric demand increased (e.g. global radiation was 13.6 MJ m⁻² on 17 July
353 compared to 23.9 MJ on 18 July while daily VPD was 0.7 kPa and 1.2 kPa, respectively) even more than the
354 sap flow. Midday sunlit leaf water potential was not distinctively different among treatments with the
355 lowest $\psi_{\text{sunlitleaf MD}}$ around -1.6 MPa throughout season. Also, G_{SMD} was rather similar among plots. The
356 $K_{\text{soil_plant MD}}$ ranged from 0.125 to 0.96 mm h⁻¹ MPa⁻¹ with a sharp reduction before harvest. In general, the
357 lowest values of $K_{\text{soil_plant MD}}$ were found in F1P2 which was consistent with the smaller overall seasonal
358 $K_{\text{soil_plant}}$ (as the slope of linear relationship between sap flow and difference of effective soil water potential
359 and sunlit leaf water potential) (see Supplementary material 5).

360 [Insert Figure 8 here]

361 The $\psi_{\text{soil_effect MD}}$ was substantially different in the two soil types and water treatments in 2018 (Figure 9a).
362 Both F1P2 and F1P3 showed a gradual drop of $\psi_{\text{soil_effect MD}}$ from 15 June until the third week of July then
363 increased after irrigation events on 18 July (Supplementary material 2b). However, $\psi_{\text{soil_effect MD}}$ of F1P2 was
364 much lower than F1P3 toward the harvest. The $\psi_{\text{soil_effect MD}}$ of F2P2 and F2P3 only decreased progressively
365 from around 10 July till harvest even though there was water supply from the irrigation (Supplementary
366 material 2b). The water applied by irrigation and coming in by rainfall were insufficient to wet up the
367 deeper soil layers which remained dry. The low G_{SMD} was corresponding to the lowest $\psi_{\text{sunlitleaf MD}}$ and



368 $K_{\text{soil_plant MD}}$ from the F1P2 (Figure 9c & 9d). The $K_{\text{soil_plant MD}}$ from all plots was ranging from 0.12 to 0.91 mm
369 $\text{h}^{-1} \text{MPa}^{-1}$. There was the drop in $K_{\text{soil_plant MD}}$ (i.e. 3 to 9 July or 17-18 July) before irrigation in this plot.
370 However, it increased after the irrigation (i.e. 10 July and 19 July). This suggests that $K_{\text{soil_plant}}$ depends
371 strongly on the soil water content and the conductivity of the rhizosphere.

372 [Insert Figure 9 here]

373 **3.2.3. Relationships of stomatal conductance, transpiration, photosynthesis with plant hydraulic** 374 **variables at the plant canopy level**

375 The slope of linear relationship between sap flow and difference of $\psi_{\text{soil_effec}}$ and $\psi_{\text{sunlitleaf}}$ is shown for three
376 consecutive days (leaf water potential measurements from the predawn) and before and after irrigation
377 applications (17, 18, and 19 July 2018 or DOY 198, 199 and 200, respectively) (Figure 10). On both DOYs
378 198 and 199, the difference between $\psi_{\text{soil_effec}}$ and $\psi_{\text{sunlitleaf}}$ was around -1.6 MPa with very low transpiration
379 rates in the treatment F1P2 which was associated with very low plant hydraulic conductance and leaf
380 curling. The whole plant hydraulic conductance was disrupted on these two days (0.06 and 0.16 mm h^{-1}
381 MPa^{-1} for DOY 198 and 199, respectively). Water was supplied on DOY 199 at 1 PM for the irrigated plots
382 (F1P3, F2P3) as well as F1P2 at 4 PM (for saving plant from death due to severe drought stress). $K_{\text{soil_plant}}$
383 was slightly changed (0.43 and 0.57 $\text{mm h}^{-1} \text{MPa}^{-1}$ for F1P3 on DOY 199 and 200, respectively and 0.5 and
384 0.58 $\text{mm h}^{-1} \text{MPa}^{-1}$ for F2P3 on DOY 199 and 200, respectively). However, the increase of $K_{\text{soil_plant}}$ was
385 substantial in the F1P2 after the irrigation. Soil water replenishment and an increase in the root - soil
386 contact (Fig. 9a) allowed the $K_{\text{soil_plant}}$ to recover overnight to 0.46 $\text{mm h}^{-1} \text{MPa}^{-1}$. This resulted in a narrower
387 water potential gradient between root zone and sunlit leaf and in a higher transpiration rate on DOY 200.

388 [Insert Figure 10 here]

389 Seasonal average of different midday hydraulic conductance components (root system hydraulic
390 conductance - $K_{\text{soil_root}}$, stem hydraulic conductance - K_{stem} , and whole plant hydraulic conductance -



391 K_{soil_plant}) are shown in Figure 11. In the same year, the K_{stem} was not much different among F1P3, F2P2, and
392 F2P3 plots. The K_{stem} of those plots was slightly higher than in the F1P2 in both years. In general, the K_{soil_root}
393 was lower than the K_{stem} . The K_{soil_root} in the F1P2 in 2018 was much lower than the remaining plots while
394 the K_{soil_root} was not much different among plots in 2017. Overall, the estimated K_{soil_plant} was around $1/$
395 $(1/K_{soil_root} + 1/K_{stem})$ regardless of soil types, years, and water treatments. Although there is a large
396 difference in total root length between two soil types (e.g. F1P3 versus F2P2), K_{soil_root} and K_{soil_plant} in those
397 two plots were not much different. The K_{soil_plant} and K_{soil_root} depend strongly on the soil water content and
398 the soil hydraulic properties. Therefore, K_{soil_plant} and K_{soil_root} were not only a plant property but also a soil
399 property.

400 [Insert Figure 11 here]

401 **3.3. Relative importance of root and leaf area growth to transpiration and crop performance at canopy** 402 **level**

403 Drought stress was observed in the rainfed plot (F2P2) in the second week of June 2017 with mild leaf
404 rolling. The crop then recovered due to sufficient rainfall and lower evaporative demand. Drought stress
405 occurring again at the stem elongation phase caused reduction of plant size (height and stem diameter)
406 (Supplementary material 4) as well as a slight reduction of leaf area and biomass in this plot
407 (Supplementary material 3a & 3c). Transpiration per unit of leaf area did not differ much among water
408 treatments and soil types in 2017 (Figure 12). The opposite was the case for the transpiration rate per unit
409 of root length. The observed root length at different soil depths (Figure 2) and total root length for two
410 plots in the stony soil was much smaller than in the silty soil (Figure 3). Therefore, transpiration per unit
411 of root length in the stony soils (F1P2 & F1P3) was almost 3 times higher than transpiration in the silty soil.
412 For the same soil, transpiration per unit root length of the irrigated treatment was slightly larger than in
413 the rainfed plot.



414 [Insert Figure 12 here]

415 The differences in sap flow per plant between water treatments and soil types were more pronounced in
416 2018 (Figure 13). The highest transpiration rate was observed in the irrigated plots (F1P3 & F2P3), followed
417 by the rainfed plot of the silty soil (F2P2) and it was lowest in the rainfed plot of the stony soil (F1P2).
418 These observations were in line with the differences in biomass and leaf area index between the
419 treatments (Supplementary material 3b & 3d) and plant size (Supplementary material 4b-c-d). In 2018,
420 severe leaf rolling was observed in the rainfed plot (F1P2) from the beginning of June until the end of the
421 growing period in 2018 (Supplementary material 3d). Similar to 2017, transpiration per unit of root length
422 was much higher in the stony plots as compared to silty plots. Also, for the silty soil, transpiration per unit
423 of root length of the irrigated plot (F2P3) was higher than in the rainfed plot (F2P2).

424 [Insert Figure 13 here]

425 Higher cumulative transpiration in the irrigated plots did not result in higher transpiration use efficiency
426 (TUE) in both soil types (Figure 14). For instance, TUE were 16.87 g mm^{-1} and 15.59 g mm^{-1} for F1P2 and
427 F2P2, respectively, while they were 15.47 and 14.79 g mm^{-1} for F1P3 and F2P3, respectively, in 2017 (Figure
428 14A). For the same soil, the rainfed plot showed slightly higher TUE than the irrigated plot. When
429 comparing the TUE of maize of the two soil types for the same water treatment, TUE at the stony soil was
430 almost the same in silty soil. The TUE was not much different among treatments and soil types in 2018.
431 Overall, TUE in 2017 was higher as compared to 2018 (Fig. 14b).

432 [Insert Figure 14 here]

433 **4. Discussions**

434 **4.1. Effects of soil types, water application, and climatic condition on root growth**

435 Our root observations showed that soil type considerably affected root growth more than water treatment
436 (Figure 2). Root growth was strongly inhibited by the stony soil where much lower root length was



437 observed than in the silty soil, especially in the deeper soil layers. This was consistent with the findings
438 reported in (Morandage et al., 2021) where a linear increase of stone content resulted in a linear decrease
439 of rooting depth across all stone contents and developmental stages. Also, both simulations and
440 observations indicated that rooting depth was sensitive to the presence of cracks in the lower
441 minirhizontron facility (Morandage et al., 2021) which could explain the high root length between 40 and
442 120 cm soil depths which was observed in the silty soil in both years. In the silty soil, root growth was
443 favored towards deeper soil layers as also reported for the same field in 2016 for winter wheat (Nguyen
444 et al., 2020). Observation in field grown maize, the higher root length density and root diameter were
445 found in the sand than in the loam. This was attributed to the higher investment in nutrient exploration
446 because the lower concentration of plant-available nutrients was in sand than in loam (Vetterlein et al.,
447 2022). Also, the larger root diameters in sand than in loam are more likely explained by the need for soil
448 contact of the roots (Jorda et al., 2022; Vetterlein et al., 2022).

449 Our total root length was in the reported range of Cai et al., (2018) who studied winter wheat roots on the
450 same soil types in 2016. The total root length in our work was higher than the reported results from Cai
451 et al., (2018) especially in the rainfed plot of the silty soil (F2P2) in 2018 (Fig. 3). In terms of the root: shoot
452 ratio, our observations were in line with those reported in the same soil types for wheat in Cai et al., (2018).
453 Ordóñez et al., (2020) has reported much larger figures of for instance 880 cm g^{-1} in different locations and
454 under different N application rates in maize growing in the Midwest of US. Jorda et al., (2022) reported a
455 wide range of root: shoot ratio from 200 to 1000 cm g^{-1} around flowering time of maize depending on the
456 wild type and root hair mutant genotypes growing on either loamy or sandy soils. More roots and higher
457 root: shoot ratios were found in the sand than in the loam in both wild type and root hair mutant
458 genotypes (Jorda et al., 2022; Vetterlein et al., 2022). Cai et al., (2018) observed much larger root: shoot
459 ratio in drought stressed plots than in irrigated plot in both soil types in winter wheat which indicated the
460 alternation of sink: source relationships to cope with water stress. This study emphasized that more



461 assimilates are used to promote root growth and extract more water under drought stress. However, this
462 was not the case for the stony soil in our work where the drought stress was more pronounced, especially
463 in 2018. A slightly higher root: shoot ratio in the F1P2 treatment compared to F1P3 (DOY 194 & 255) was
464 observed in 2017 while the root: shoot ratio in the two treatments was almost the same on DOY 199 and
465 228 in 2018 (Fig. 3). We only observed much higher root: shoot ratio in the rainfed plot (F2P2) as compared
466 to the irrigated plot on the silty soil (F2P3). Comas et al., (2013) has reported that maize increases the ratio
467 of root to leaf surface area and relative distribution to deeper depths in responses to water deficit. Under
468 drought stress, root growth of maize continues longer into the season than shoot and vegetative growth
469 and even beyond the onset of reproduction. A drop of soil water potential (Supplementary material 2b),
470 thus effective soil water potential (Figure 8a) was substantial from 10th July 2018 toward the harvest in the
471 rainfed plot in the silty soil (F2P2) which was consistent with the reduction of leaf water potential (Fig. 8b),
472 leaf area (Supplementary material 3c), total dry matter (Supplementary material 3d), and crop height
473 (Supplementary material 4b) as compared the irrigated plot (F2P3). This indicates a mild water stress in
474 2018 in the rainfed plots on the silty soil. The larger root: shoot ratio in this F2P2 plot in 2018 as compared
475 to F2P3 could be explained by the change of source: sink relations where more assimilates were devoted
476 to root growth, even at a later growth stage. Moreover, the low stone content and soil cracks (Morandage
477 et al., 2021) might favor root growth in the deeper soil layers which are close to the lower soil water table
478 in the site with silty soil (Vanderborgh et al., 2010).

479 **4.2. Effects of soil types, water application, and climatic condition on stomatal conductance,** 480 **photosynthesis, transpiration, leaf water potential, and plant hydraulic conductance**

481 **4.2.1. Leaf water potential and stomatal conductance as affected soil water conditions**

482 In our study, stomata closed earlier and at more negative soil and leaf water potentials in stony soil than
483 in silty soil (see Fig. 4, 5, 6 and 7). In other work, Koehler et al., (2022) reported that maize stomata closed
484 at lower negative leaf water potentials in sand than in loam growing under controlled environment. Cai et



485 al., (2022b) investigated transpiration response of pot-grown maize in two contrasting soil textures (sand
486 and loam) and exposed to two consecutive VPD levels (1.8 and 2.8 kPa). Transpiration rate decreased at
487 less negative soil matric potential in sand than in loam at both VPD levels. In sand, high VPD generated a
488 steeper drop in stomatal conductance with decreasing leaf water potential which indicated the
489 transpiration and stomatal responses depend on soil hydraulics.

490 Stomatal control is an early and effective response to water stress to prevent the plant from water loss
491 and dehydration. Maize is considered as an isohydric plant which closes its stomata to maintain leaf water
492 potential above critical levels (Tardieu and Simonneau, 1998). Our results showed that minimum leaf
493 water potential varied among treatments (-1.5 MPa for F1P3, F2P2, and F2P3 and up to -2 MPa for F1P2
494 in 2017, while in 2018 minimum values were -2 MPa for F2P3, F2P2, and F2P3 and -2.7 MPa for F1P2) (Fig.
495 7 and Fig. 8, Fig. 9). Large variability of minimum LWP has been reported for maize genotypes. Leaf water
496 potential can be limited at quite high values, for instance -0.8 MPa in some lines of maize, while values as
497 low as -1.5 MPa have also been recorded (Welcker et al., 2011). Some drought-tolerant maize genotypes
498 close stomata at less negative leaf water potential under soil water depletion than more sensitive ones,
499 which is associated with their ability to avoid xylem embolism and hydraulic failure (Cochard, 2002; Tyree
500 et al., 1986; Li et al., 2009). However, our results show that the leaf water potential threshold can vary
501 within the same genotype depending on soil types, climatic conditions and water management. It should
502 be noted the constant ψ_{leaf} level (around -1.8 MPa) under different soil water regimes reported in Tardieu
503 and Simonneau (1998) that was associated with high VPD values, was based on observations from a single
504 day. Measurements on ψ_{leaf} and G_s for different days during several growing seasons have been rarely
505 reported for maize. The results of our study confirmed that maize appears to maintain its ψ_{leaf} at around -
506 1.5 to -2 MPa which depended on evaporative demand and levels of soil moisture (Fig. 1, Fig. 7, Fig. 8, and
507 Fig. 9). This has been reported recently in Nguyen et al. (2022a). Our current study, which investigates the
508 drivers of the modifications of ψ_{leaf} during the growing season, also confirmed that such stomatal



509 regulation and the ψ_{leaf} were mediated by soil hydraulics. Cochard, (2002) reported that stomatal closure
510 is complete between -1.6 and -2 MPa. In our study, the observed ψ_{leaf} was below -2 MPa for several days.
511 Similar values were also reported by Li et al. (2002) for field-grown maize in semiarid conditions. In our
512 study, leaf water potential dropped below -2 MPa in the rainfed plots to levels much lower than those
513 observed in the irrigated plots in 2018. This could imply different degrees of isohydry in maize. A
514 continuum exists in the degree to which stomata regulate the ψ_{leaf} for trees (Domec and Johnson, 2012;
515 Klein, 2014) or in grape-vine (Schultz, 2003). Also, cultivars of grape vine show large differences in
516 minimum ψ_{leaf} indicating differing degrees of isohydric behavior (Coupel-Ledru et al., 2014). When
517 comparing different herbaceous species, Turner et al., (1984) showed that there was a range of isohydric
518 behavior among the species in terms of the response to increasing vapor pressure deficit (VPD) under
519 sufficient soil moisture. However, conclusions concerning contrasting minimum ψ_{leaf} between 2017 and
520 2018 should not be overemphasized. Observed extremely low ψ_{leaf} correspond with the extremely low Gs
521 and were further accompanied by complete leaf curling in rainfed treatment under stony soil in 2018 (Fig.
522 4, 5, and Fig. 9) due to the extremely dry and hot summer and severe soil dryness.

523 **4.2.2. Hydraulic conductance components as affected by soil water conditions**

524 Estimates of hydraulic components in soil-plant-atmosphere continuum are important not only to
525 understand its underlying relationship to other crop characteristics (stomatal conduction, transpiration,
526 and photosynthesis) but also to provide modeling parameters in process-based soil-root-shoot models
527 (Nguyen et al., 2020; Sulis et al., 2019; Nguyen et al., 2022b). Measurement of the components of hydraulic
528 conductance are challenging under field conditions because it requires the estimate of transpiration and
529 root to leaf water potential gradients. To our knowledge, our results were unique with regard to the
530 dynamics of $K_{\text{soil_plant}}$ for field-grown maize on two soil types and under contrasting water, and climate
531 conditions. Our seasonal $K_{\text{soil_plant}}$ ranged from 0.12 mm h⁻¹ MPa⁻¹ to 0.9 mm h⁻¹ MPa⁻¹ (Fig. 8 & Fig. 9; Fig.
532 10, and Supplementary material 5). Root system hydraulic conductance ranged from 0.26 to 1.47 mm h⁻¹



533 MPa⁻¹ (Figure 11). Note that the unit of $K_{\text{soil_plant}}$ as mm h⁻¹ MPa⁻¹ could be equivalent to the unit of 10⁻⁵ h⁻¹
534 ¹ if one assumes 1MPa is approximately 10⁵ mm in terms of pressure head. Cai et al., (2018) reported root
535 hydraulic conductance in winter wheat from 0.05 x 10⁻⁵ h⁻¹ to 0.5 x 10⁻⁵ h⁻¹ in two similar soil types. Nguyen
536 et al., (2020) also reported $K_{\text{soil_plant}}$ in winter wheat from 0.0625 x 10⁻⁵ h⁻¹ to 0.461 x 10⁻⁵ h⁻¹. Meunier et al.,
537 (2018) focused on estimating the root system hydraulic conductance of maize in a container experiment
538 where the range of $K_{\text{soil_plant}}$ was much larger from 0.37 x 10⁻⁵ h⁻¹ to 36 x 10⁻⁵ h⁻¹ for the plant density of 10
539 plant m⁻². Jorda et al., (2022) estimated root system hydraulic conductance of 0.5 to 1.5 10⁻³ d⁻¹ which
540 would be roughly between 2 to 6 10⁻⁵ h⁻¹. To simulate leaf water potential in the modeling work for field
541 maize, Nguyen et al., (2022b) based on assumption that $K_{\text{soil_plant}}$ was 0.53 x $K_{\text{soil_root}}$. Such fraction (0.53) was
542 consistent with the reported range in our work (0.3-0.8) with average $K_{\text{soil_plant}}$ was at half of root system
543 hydraulic conductance across treatments. In our work, except the F2P2 in 2018, the stem hydraulic
544 conductance was 10% to 60% higher than root system hydraulic conductance. Gallardo et al., (1996)
545 reported that stem hydraulic conductance of wheat was lower than root system conductance at around
546 71 to 91 days after sowing (DAS), but they were similar at 102 DAS. In lupine, stem hydraulic conductance
547 was two times higher than root system conductance regardless of measured days. The larger root length
548 in wheat than lupine did not necessarily result in higher root conductance in wheat. Together with this
549 study, our study emphasizes the values of stem hydraulic conductance compared to the root hydraulic
550 conductance in maintaining water potential gradient from shaded leaf or plant color to the sunlit leaf.

551 Our results showed clear differences in $K_{\text{soil_plant}}$ among treatments where much lower $K_{\text{soil_plant}}$ was
552 observed in the F1P2 as compared to F2P2 (see Figure 10 for 2018; Figure 8 and 9 and Supplementary
553 material 5 for both years). This indicated the soil texture dependence for whole plant hydraulic
554 conductance. Maize plants with the shorter root system (i.e. rainfed plot in the stony soil in 2018) (Fig. 3)
555 had lower plant hydraulic conductance. Our results indicated that there was an impact of soil hydraulic
556 conditions on $K_{\text{soil_plant}}$ via the reduction of root system hydraulic conductance. Our analysis for three



557 consecutive measurement days in 2018 (Fig 10) showed that in the silty soil, K_{soil_plant} decrease when soil
558 water potentials are becoming more negative. For instance, in the silty soil in 2018 when the soil water
559 potentials were considerably lower in the rainfed than in the irrigated plot (e.g. after 10th July), K_{soil_plant}
560 was lower in the rainfed than in the irrigated plot. In the stony soil, the K_{soil_plant} and leaf water potentials
561 seems to decrease more considerably (compared to the silty soil) when the soil water potentials become
562 more negative. In other words, K_{soil_plant} increased considerably when the soil water potentials in the stony
563 soil increased. Koehler et al., (2022) analyzed the maize plant responses to soil drying under controlled
564 climate conditions with three soil types (sand, sandy loam, and loam). This study confirmed the impact of
565 soil texture on plant response to soil drying in various relationships. In their work, the soil-plant
566 conductance decreased in both sand and loam but at less negative water potentials in the sand than in the
567 loam. Root system hydraulic conductance decreased at less negative bulk soil water potential in the coarse
568 soil than in the fine soil (Vanderborgh et al., 2023). In our work, K_{soil_plant} increased slowly after irrigation
569 mainly for the severe water stress plot (see F1P2 on 19 July in Fig 9d and 10c). This implied that added soil
570 water by irrigation took some time for recovery the soil-root contact within the rhizosphere.

571 **4.2.3. Relationships of stomatal conductance, transpiration, photosynthesis with plant hydraulic**
572 **variables**

573 In 2017, our estimated midday effective soil water potential ($\psi_{soil_effecMD}$) did not vary much (between soil
574 types and treatments) which was consistent with the low variability in midday sunlit leaf water potential
575 ($\psi_{sunlitleafMD}$) and K_{soil_plant} among water treatments (Fig. 8). The $\psi_{soil_effecMD}$ was high (around -0.35 MPa)
576 while $\psi_{sunlitleafMD}$ was around -1.5 MPa (Fig. 8c). In contrast, the difference of $\psi_{soil_effecMD}$, $\psi_{sunlitleafMD}$, and
577 K_{soil_plant} was higher among water treatments and soil types in 2018 as compared to 2017. Moreover, the
578 high VPD and air temperature in combination with the small precipitation in the main growing season in
579 2018 led to a stronger reduction of $\psi_{soil_effecMD}$ up to -0.75 MPa (i.e. in F1P2 in the stony soil on 17 and 18
580 July in 2018, Figure 9) and $\psi_{sunlitleafMD}$ to -2.5 MPa. This low $\psi_{soil_effecMD}$ in F1P2 was associated with low



581 stomatal conductance (Fig. 9c), low $K_{\text{soil_plant}}$ (Fig. 9d), and strong transpiration reduction (Fig. 10a-b, Fig.
582 12, and Supplementary material 5). Our results were in line with the analysis from Cai et al., (2022a) which
583 revealed that water uptake depended on effective soil water potential which in turn depended on soil
584 water potential which differed between plots with different textures.

585 The transpiration rate and $K_{\text{soil_plant}}$ (slope of linear regression lines in Fig. 10a and b) were very low in the
586 rainfed plot under the stony soil (F1P2) which was associated with the large $\psi_{\text{difference}}$ (Fig. 10a & b) and the
587 lower stomatal conductance as compared to other plots (Fig. 9c). The $K_{\text{soil_plant}}$ slightly increased after
588 irrigation (DOY 199 in Fig. 10b) corresponding with the smaller $\psi_{\text{difference}}$ (Fig. 10b) and an increase in
589 stomatal conductance (Fig. 9c). Seasonal $K_{\text{soil_plant}}$ was low in the rainfed plot under stony soil (F1P2) with
590 the larger $\psi_{\text{difference}}$ (Supplementary material 5). In addition, our study showed that the midday stomatal
591 conductance, photosynthesis, and transpiration were significantly correlated only with midday $K_{\text{soil_plant}}$ in
592 the rainfed plot on the stony soil (F1P2) in 2018 where high VPD and temperature occurred
593 (Supplementary material 6, 7, and Supplementary material 8). Maize plant had lower plant hydraulic
594 conductance in the rainfed plot in stony soil required the larger gradients in soil water pressure to sustain
595 the same transpiration rate (thus exhibited earlier stomatal closure) as compared to the same plot in the
596 silty soil. This was in line with a study from Abdalla et al., (2022) which suggested that during soil drying,
597 stomatal regulation of tomato is controlled by root and soil hydraulic conductance. Recent work from
598 Müllers et al., (2022) on faba bean and maize suggested that differences in the stomatal sensitivity among
599 plant species can be partly explained by the sensitivity of soil-plant hydraulic conductance to soil drying.
600 The loss of conductance has immediate consequences for leaf water potential and the associated stomatal
601 regulation. Cai et al., (2022b) also showed that the decrease in sunlit leaf stomatal conductance was well
602 correlated with the drop in soil-plant hydraulic conductance, which was significantly affected by soil
603 texture. This was confirmed in our work where the stony soil strongly impacted on root growth, modulated
604 $K_{\text{soil_plant}}$, and consequently influenced the leaf stomatal conductance, photosynthesis, and transpiration.



605 **4.3. Relative contribution of water control by leaves and roots on transpiration and transpiration use**
606 **efficiency**

607 Responses of crops via stomatal control to reduce water loss at leaf scale while maintaining leaf
608 photosynthesis and water use efficiency were reported earlier (Nguyen et al., 2022a; Vitale et al., 2007).

609 In addition to that, in the maize experiments in 2017 and 2018 leaf rolling was observed in both rainfed
610 plots on the stony and the silty soil in the second week of June 2017 and from the beginning of June until
611 the end of the growing period in 2018. This indicates another dehydration avoidance mechanism resulting
612 from morphological adjustments which is an effective mechanism for delaying senescence (Aparicio-Tejo
613 and Boyer, 1983; Richards et al., 2002). Stomatal closure resulted in more reduction of transpiration and
614 assimilation in the rainfed plots than irrigated plots with the same soil type (Fig. 5, Fig. 6, Fig. 7, and Fig.
615 13A). There was reduction of shoot biomass (also stem size and leaf size adjustments) in F1P2 as compared
616 to other plots. However, the TUE was not smaller in this plot than the remaining plots. These observations
617 confirm that plant size adjustments through reduction of height, leaf width and length are efficient
618 responses to reduce water loss at canopy scale in addition to stomatal control at the leaf level.

619 Relative contribution of leaf area to transpiration has been highlighted in wheat where reduction of tiller
620 number resulted in significantly (lower LAI, thus lower canopy transpiration (Cai et al., 2018; Trillo and
621 Fernández, 2005; Nguyen et al., 2022a). However, root system conductance per unit of leaf area and per
622 unit root mass were strongly reduced and eventually more than reduction of leaf area under water stress
623 (Trillo and Fernández, 2005). In our work, expressing the transpiration per unit of root length on the one
624 hand allowed to analyze the role of total root length to water uptake. However, on the other hand, the
625 lower total root length did not necessarily result in a lower root water uptake and vice versa. For instance,
626 the rainfed plot of the treatment F2P2 had the larger total root length which could postpone the effect of
627 soil water limitations in drying soils due to greater ability to extract water from subsoils. Therefore,
628 transpiration was very similar between F2P2 and F2P3. Despite of the much lower total root length in the



629 stony soil, $K_{\text{soil_plant}}$ in the irrigated plot (F1P3) was not much lower than in the same water treatment in
630 the silty soil (F2P3, Fig. 8c, 9c, Fig. 10, and Supplementary material 5). This could be explained by the fact
631 that the $K_{\text{soil_plant}}$ variability was not only depended on root architecture (here the root length and
632 distribution) but also depended on the variability of root segment hydraulic properties which has also been
633 illustrated and discussed in Zwieniecki et al. (2002), Frensch and Steudle (1989), Meunier et al. (2018),
634 Couvreur et al. (2014), and Ahmed et al. (2018). Meunier et al. (2020) showed that more than 65% of the
635 variability of root system conductance of maize plants could be attributed to variability in root
636 architecture, which includes root length, whereas only 25% of the variability was attributed to root
637 segment hydraulic properties. However, the analysis of Meunier et al., (2020) neither included the impact
638 of root hairs nor the impact of rhizosphere conductivity but only focused on the root system hydraulic
639 conductance. Moreover, the contribution of shoot hydraulic conductance could be large in plants (Gallardo
640 et al., 1996; Trillo and Fernández, 2005; Sunita et al., 2014) which also confirmed in our work. In our work,
641 $K_{\text{soil_plant}}$ comprised root and shoot conductance which are directly influenced by soil hydraulics. Our
642 estimates of $K_{\text{soil_plant}}$ varied with transpiration and gradients of $\psi_{\text{sunlitleaf}}$ and $\psi_{\text{soil_effec}}$. Thus, any change of
643 soil hydraulic conductance will change the root to shoot water potential. Consequently, it will affect the
644 gradients between shoot and root rhizosphere (Carminati and Javaux, 2020). Thus, our study is revealing
645 the importance of both soil texture characteristics and root phenotypic traits (here root length) in
646 regulating plant transpiration (Cai et al., 2022a). Other traits like root hair density (Cai et al., 2022a) or
647 higher root length density (Vadez, 2014) could contribute to the soil to root water potential and root-zone
648 hydraulic conductance where dense root hairs are delaying soil water deficit in drying soils. However,
649 contrast results have shown that root hairs did not have an effects on root water uptake (see Jorda et al.
650 2022). The role of root hairs could not be analyzed in our work which based on the root data from
651 minirhizotron images.

652 5. Conclusion



653 We presented plant hydraulic characteristics and crop growth from root to shoot of maize under field-
654 grown conditions with two soil types (silty and stony), each soil with two water regimes (irrigated and
655 rainfed) for two growing seasons (2017, 2018). Our results confirmed that root length and root: shoot ratio
656 was modulated by soil types and water treatment but less by seasonal evaporative demand. Increase root:
657 shoot ratio has been an important response of maize that allows plants to extract more water under
658 drought stress that occurred rather in the silty soil but less in the stony soil due to the higher content of
659 stony material. Despite of lower root length in the stony irrigated plot, transpiration rate was not much
660 lower than in the silty irrigated plot. This could be related to another property of the root such as root
661 segment conductance or other root traits (e.g. root hair). Further investigation with extensive
662 measurements of roots including axial and radial root conductance at field scale will be required to better
663 explain the observed results.

664 Another conclusion is that stomatal regulation maintains leaf water potential at certain thresholds which
665 depends on soil types, soil water availability, and seasonal atmospheric demand. The stomata conductance
666 was smaller and at more negative leaf water potentials in stony soil than in silty soil. The leaf water
667 potentials are affected by the soil-plant hydraulic conductance. In addition to stomatal regulation,
668 leaf growth and plant size adjustments are important to regulate the transpiration that water use
669 efficiency was not different among treatments and soil types in the same year.

670 The lowest soil-plant hydraulic conductance was observed in the stony soil with severe drought stress as
671 compared to silty soil while its variation depends also on the soil water variation (before and after
672 irrigation). Root system and soil-plant hydraulic conductance depended strongly on soil hydraulic
673 properties. In the stony soil, which has a considerably smaller water holding capacity than the silty soil,
674 root length was considerably smaller than in the silty soil. Nevertheless water uptake per unit root length
675 was much larger than in the fine soil. This also means that the hydraulic conductance per unit root length
676 must have been much larger in the stony soil than in the fine soil. Cai et al., (2018) observed a similar effect



677 for winter wheat but they found much smaller differences in the root length normalized root conductance.
678 The higher root length normalized root conductance means that the anatomy of the root tissues must
679 have been influenced by the soil texture and compensated the considerably smaller root length in the
680 stony soil. Looking at the effect of water treatments in the silt soil, the non-irrigated plot had more roots
681 than the irrigated one and both had more roots in the year with high VPD. But the soil-root conductance
682 was higher in the irrigated plot than in the rainfed plot. This means that in the irrigated plot, the soil-root
683 conductance per unit root length was higher than in the rainfed plot. This could either be due to wetter
684 soil conditions and higher soil conductance or it could be due to a larger conductance of the root tissues.
685 Especially in 2017 when the silty soil was wetter, the slightly larger soil-root conductance in the irrigated
686 plot is most likely the result of larger root tissue conductance in the irrigated plot. Thus, how root
687 architecture (here represented simply by the total root length) and root tissue conductivities 'respond' to
688 drought stress might be opposite depending on the comparisons that are made. When the stony soil and
689 silt soil are compared, the higher 'stress' due to lower water availability in the stony soil resulted in less
690 roots with a higher root tissue conductance in the soil with more stress. When comparing the rainfed with
691 the irrigated plot in the silty soil, the higher stress in the rainfed soil resulted in more roots with a lower
692 root tissue conductance in the treatment with more stress. This illustrates that the 'response' to stress can
693 be completely opposite depending on conditions or treatments that lead to the differences in stress that
694 are compared. Therefore, it cannot be the 'stress' alone that defines how a plant will react and adapt its
695 root system. Modelling the impact of stress and the feedback between drought stress and plant
696 development is likely controlled by other properties or parameters that change with changing soil water
697 availability and atmospheric water demand than the plant stress level. Results from this study show that
698 soil-crop models should focus not only on simulating stomatal regulations to capture the response to
699 drought stress, but also require adequate representations of leaf growth and adjustments.

700



701 **List of Tables**

702 Table 1. Crop phenology and management information for different treatments in 2017 and 2018.

	2017				2018			
Soil types	Stony (F1)	Stony (F1)	Silty (F2)	Silty (F2)	Stony (F1)	Stony (F1)	Silty (F2)	Silty (F2)
Water treatments	Rainfed (P2)	Irrigated (P3)	Rainfed (P2)	Irrigated (P3)	Rainfed (P2)	Irrigated (P3)	Rainfed (P2)	Irrigated (P3)
Plot names	F1P2	F1P3	F2P2	F2P3	F1P2	F1P3	F2P2	F2P3
Growing season (days) [‡]	136	136	136	136	107	107	107	107
Cumulative rainfall (mm) [*]	248.7	248.7	248.7	248.7	91.3	91.3	91.3	91.3
Irrigation (mm)	0	130	0	130	66	257.6	0	257.6
Fertilizer application (mm/dd) (per hectare)	05/09: 100 kg N + 40kg P ₂ O ₅ 07/06: 80 kg N + 40 kg K ₂ O				05/22: 100 kg N 05/30: 40 kg P ₂ O ₅ + 40 kg K ₂ O 06/27: 80 kg N			
Sowing date (mm/dd)	05/04				05/08			
Emergence date	05/09				05/13			
Tasseling date	07/09				07/09			
Silking date	07/14				07/11			
Harvest date	09/12				08/22			

703 Notes: [‡] from sowing to harvest; ^{*} for rainfall for whole growing season;



List of Figures

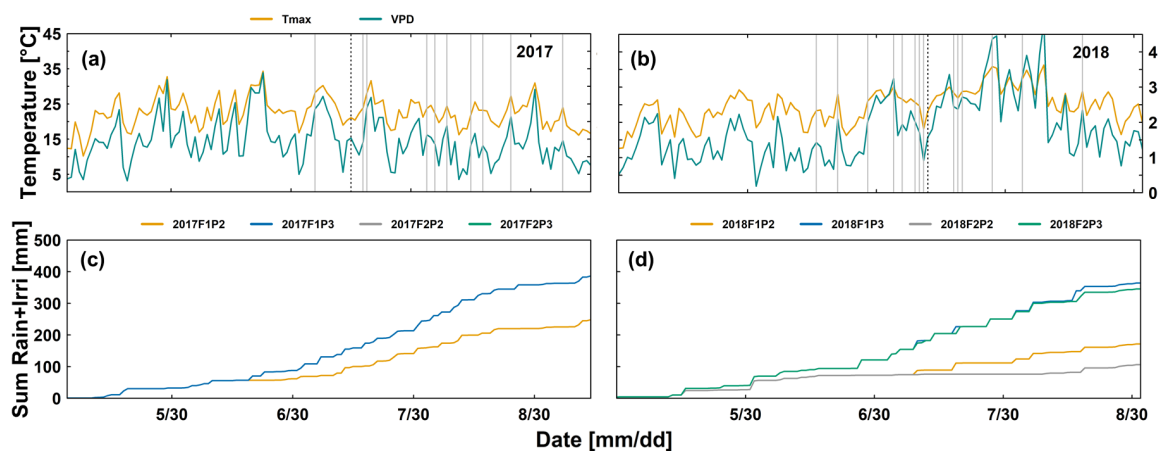


Figure 1: Daily maximum air temperature (Tmax) (°C), daily maximum air vapor pressure deficit (VPD) (kPa) in the two growing seasons (a) 2017 and (b) 2018 and cumulative (sum) of rainfall and irrigation from the rainfed (P2) and irrigated (P3) plots of the stony soil (F1) and silty soil (F2) in the two growing seasons (c) 2017 and (d) 2018. The black dashed vertical lines (a) and (b) indicate silking time. Grey vertical lines in (a) and (b) indicate the measured days for leaf gas exchange and leaf water potential. Two lines for 2017F2P2 and 2017F2P3 were overlapped by the lines from 2017F1P2 and 2017F1P3, respectively

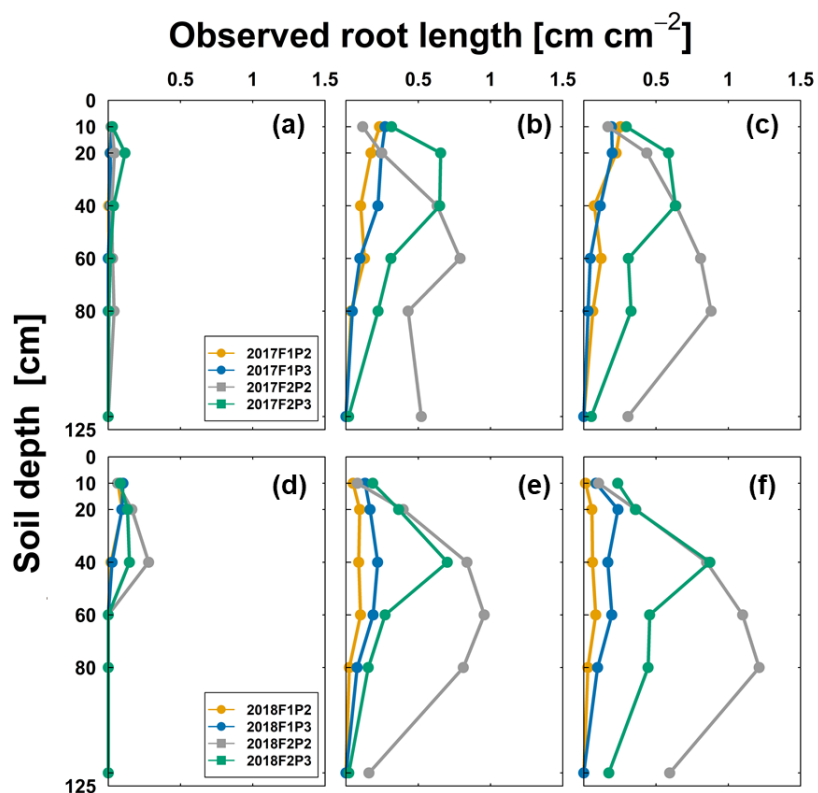


Figure 2: Observed root length from minirhizotubes (cm cm^{-2}) from 10, 20, 40, 60, 80, and 120 cm soil depth from the rainfed (P2) and irrigated (P3) plots of the stony soil (F1) and silty soil (F2) in the two growing seasons in 2017 (a - 8 June, b - at silking on 13 July, c - at harvest on 12 September) and in 2018 (d - 7 June, e - at one week after silking - 18 July, f - one week before harvest - 16 August).

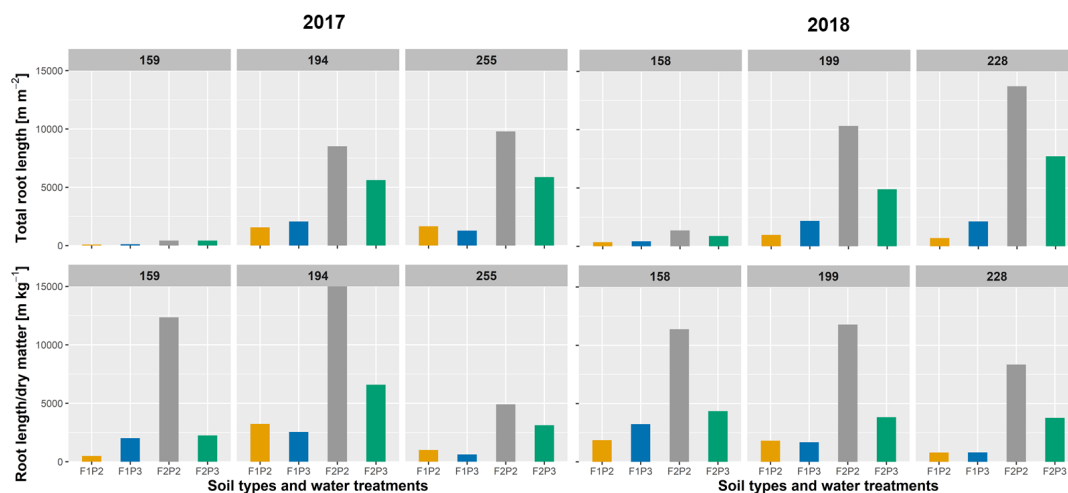


Figure 3: Observed root length from minirhizotubes (m m^{-2}) and ratio of root length per shoot dry matter (m kg^{-1}) from the rainfed (P2) and irrigated (P3) plots of the stony soil (F1) and silty soil (F2) in the two growing seasons (DOY 159, 194, and 255, left panel) in 2017 and in 2018 (DOY 158, 199, and 228, right panel) where on 8 June (DOY 159) at silking on 13 July (DOY194) 2017; and at harvest on 12 September (DOY 255) in 2017; 7 June (DOY 158), one week after silking on 18 July (DOY 199); and one week before harvest on 16 August (DOY 228) in 2018 (see also Figure 2).

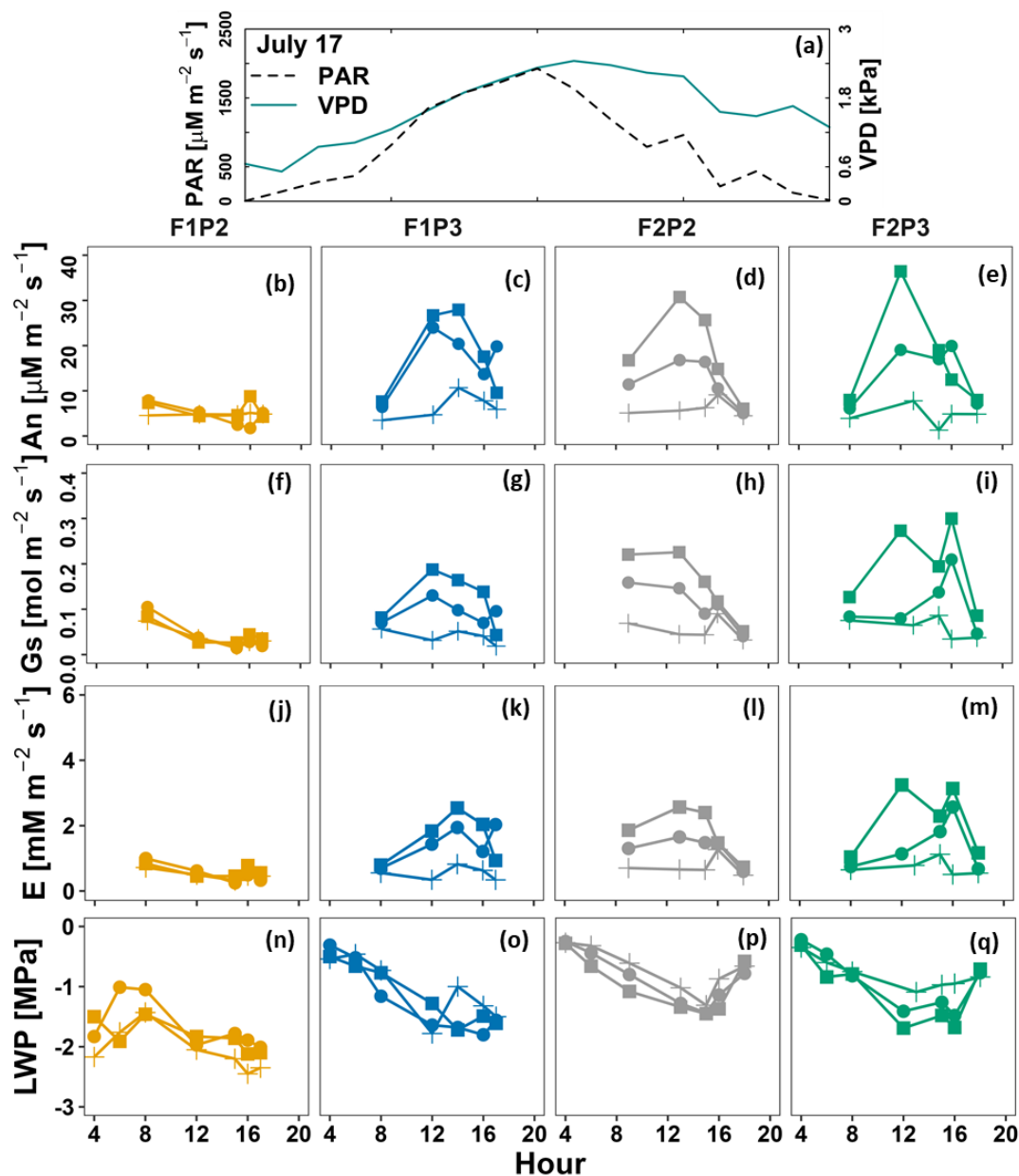


Figure 4. Diurnal course of (a) photosynthetically active radiation (PAR) and vapor pressure deficit (VPD), (b–e) leaf net photosynthesis (An), (f–i) leaf stomatal conductance (Gs), (j–m) leaf transpiration (E), and (n–q) leaf water potential (LWP) on 17 July in maize in 2018 before irrigation at the rainfed (P2) and irrigated (P3) plots of the stony soil (F1) and silty soil (F2). Measurement was carried out from shaded leaf (plus symbol with lines) and two sunlit leaves (solid dot - lines and solid square - lines).

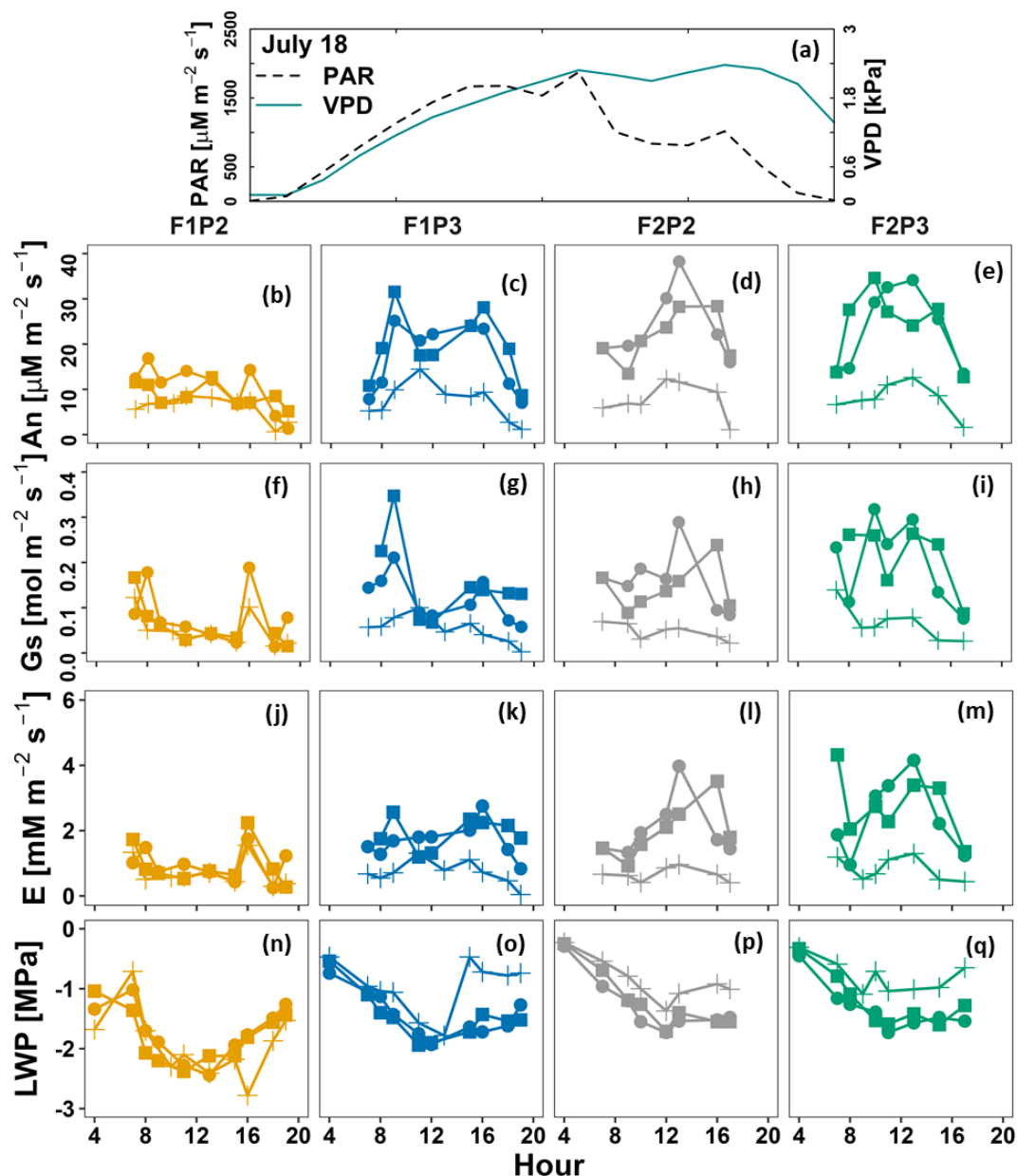


Figure 5. Diurnal course of (a) photosynthetically active radiation (PAR) and vapor pressure deficit (VPD), (b–e) leaf net photosynthesis (An), (f–i) leaf stomatal conductance (Gs), (j–m) leaf transpiration (E), and (n–q) leaf water potential (LWP) on 18 July in maize in 2018 before irrigation at the rainfed (P2) and irrigated (P3) plots of the stony soil (F1) and silty soil (F2). Measurement was carried out from shaded leaf (plus symbol with line) and two sunlit leaves (solid dot - lines and solid square - lines). Crop was irrigated at 1 PM, 1 PM, 4 PM for F1P3, F2P3, and F1P2, respectively (22.75 mm for each plot) (Supp. 2).

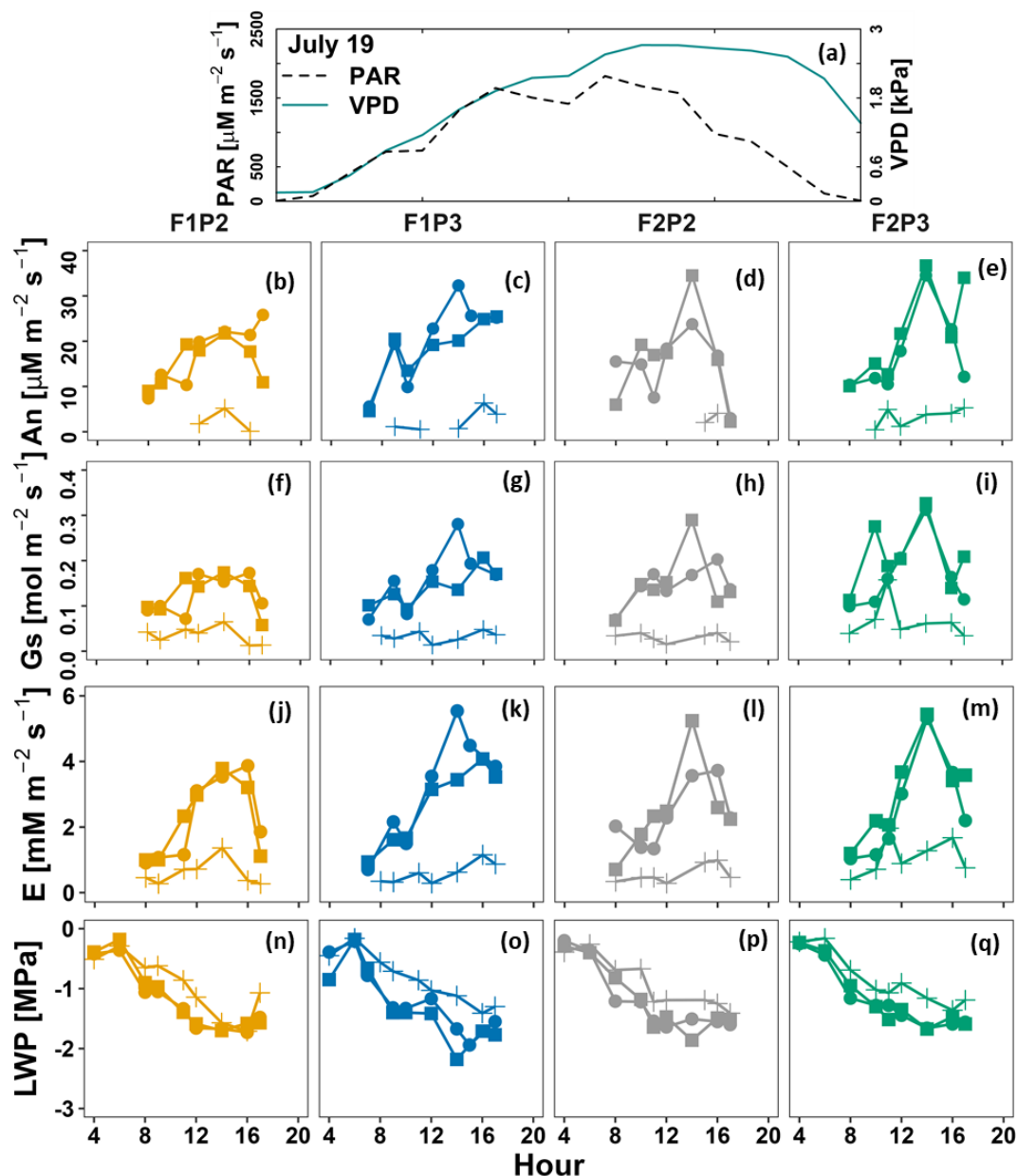


Figure 6. Diurnal course of (a) photosynthetically active radiation (PAR) and vapor pressure deficit (VPD), (b–e) leaf net photosynthesis (An), (f–i) leaf stomatal conductance (Gs), (j–m) leaf transpiration (E), and (n–q) leaf water potential (LWP) on 19 July in maize in 2018 after irrigation at the rainfed (P2) and irrigated (P3) plots of the stony soil (F1) and silty soil (F2). Measurement was carried out from shaded leaf (plus symbol with line) and two sunlit leaves (solid dot - lines and solid square -lines). Crop was irrigated on 18 July at 1 PM, 1 PM, 4 PM for F1P3, F2P3, and F1P2, respectively (22.75 mm for each plot) (Supp. 2).

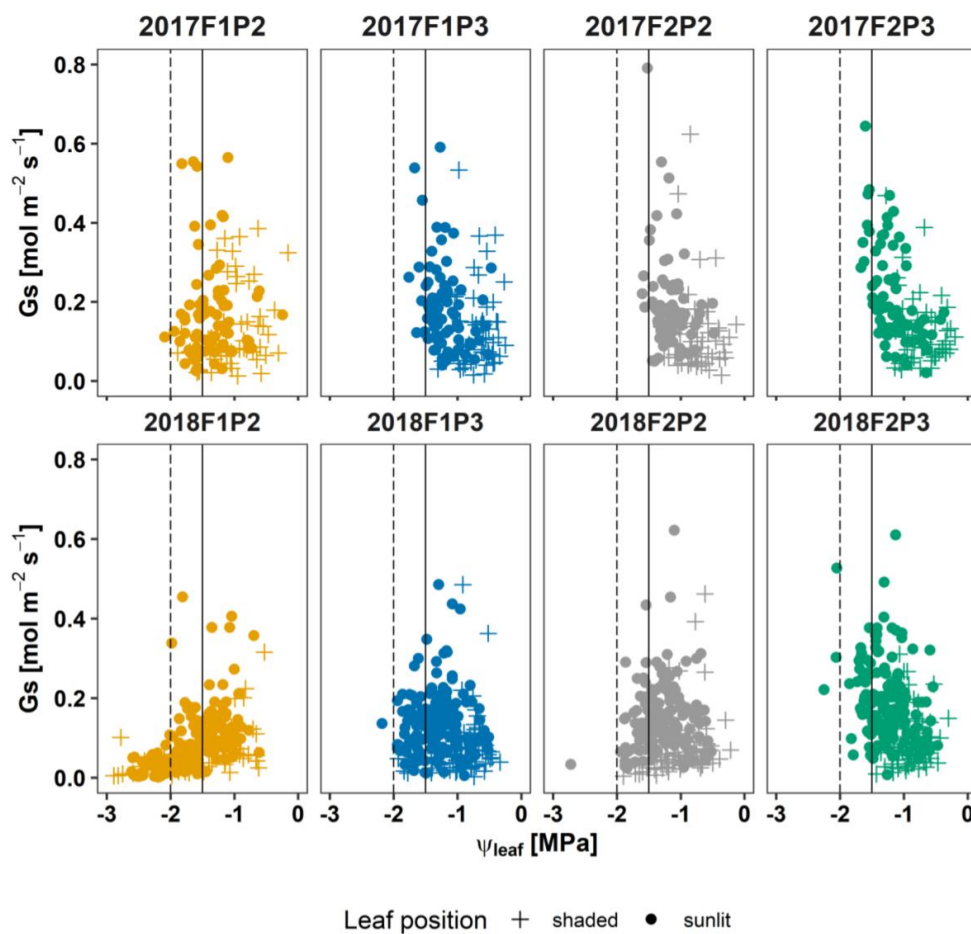


Figure 7: Seasonal stomatal conductance to water vapor (G_s) versus leaf water potential (ψ_{leaf}) in 2017 (top panel) and in 2018 (bottom panel) at the rainfed (P2) and irrigated (P3) plots of the stony soil (F1) and silty soil (F2). Vertically continuous and dashed lines indicated ψ_{leaf} at -1.5 and -2 MPa, respectively. Measurement was carried out from shaded leaf (plus symbol) and two sunlit leaves (solid dots)

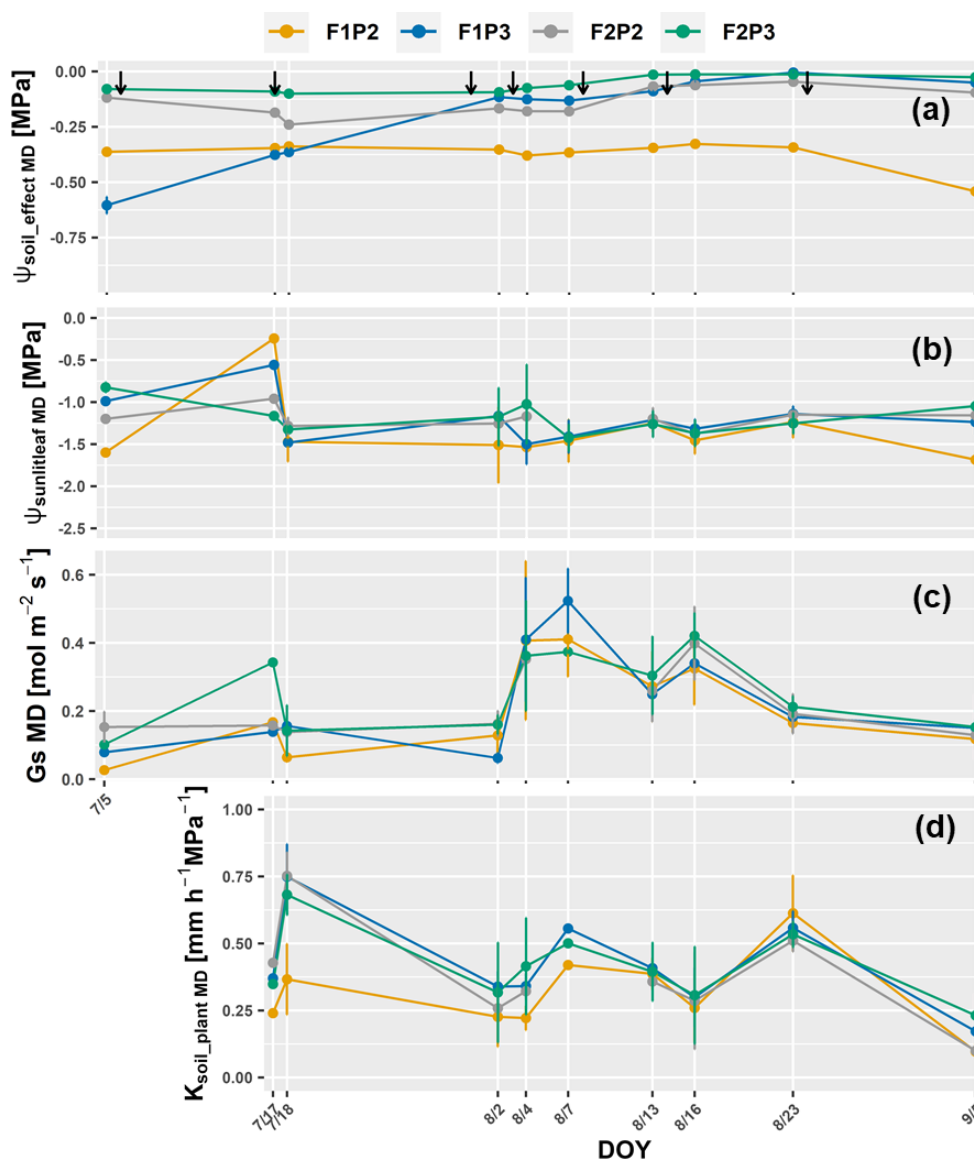


Figure 8: Dynamic of around midday (MD) of (a) the effective soil water potential ($\psi_{\text{soil_effec, MD}}$) (b) sunlit leaf water potential ($\psi_{\text{sunlitleaf MD}}$), (c) stomatal conductance (Gs MD) and (d) whole soil-plant hydraulic conductance ($K_{\text{soil_plant MD}}$) in the growing season 2017 from the rainfed (P2) and irrigated (P3) plots of the stony soil (F1) and silty soil (F2). Error bars indicate the standard deviation of the different values taken around midday (11 AM, 12AM, 1PM, and 2 PM) of different sunlit leaves. Whole soil-plant hydraulic conductance was shown from 17 July when sap flow was measured. The black arrows indicates the irrigation events for the irrigated treatments F1P3 and F2P3 in the showing period.

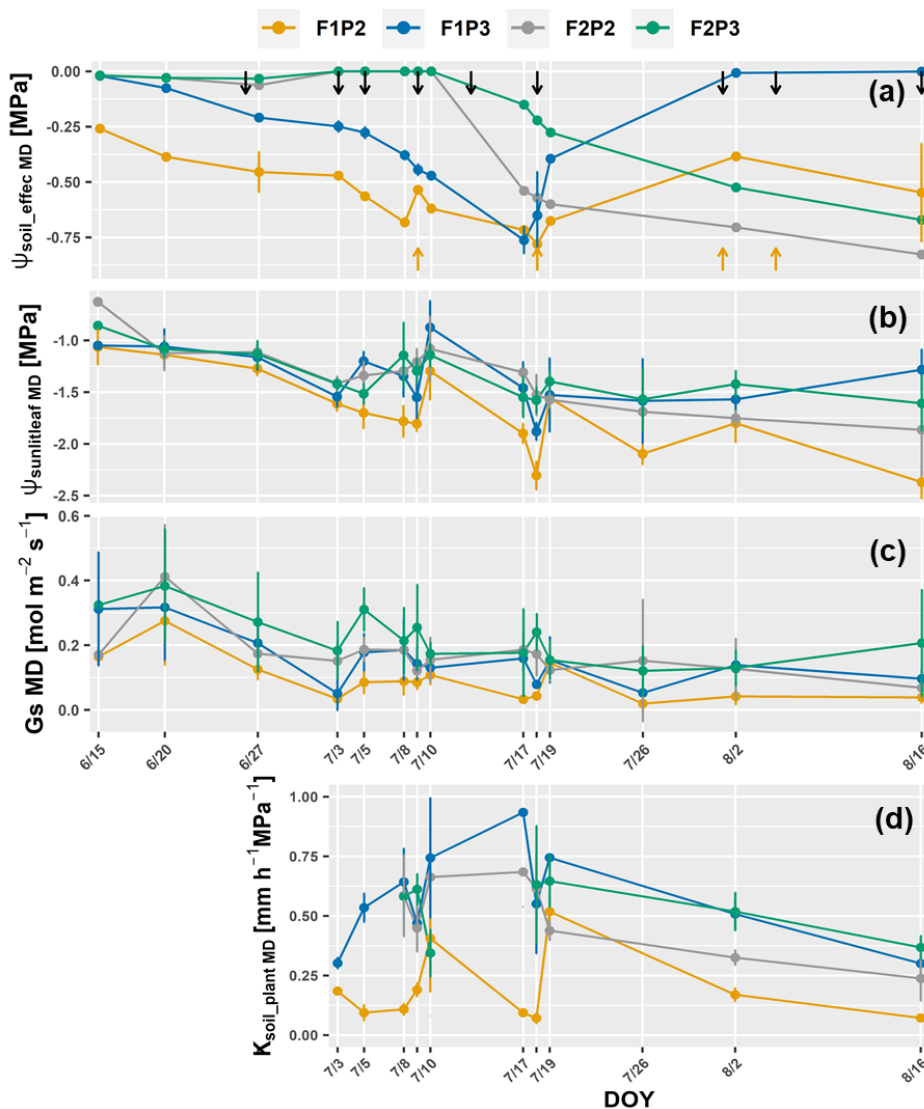


Figure 9: Dynamic of around midday (MD) of (a) the effective soil water potential ($\Psi_{soil_effec\ MD}$) (b) sunlit leaf water potential ($\Psi_{sunitleaf\ MD}$), (c) stomatal conductance ($G_s\ MD$) and (d) whole soil-plant hydraulic conductance ($K_{soil_plant\ MD}$) in the growing season 2018 from the rainfed (P2) and irrigated (P3) plots of the stony soil (F1) and silty soil (F2). Error bars indicate the standard deviation of the different values taken around midday (11 AM, 12AM, 1PM, and 2 PM) Leaf water potential and stomatal conductance were 2 sunlit leaves and one shaded leaf at each measured hour. Whole soil-plant hydraulic conductance was shown from 3 July when sap flow was measured. The black arrows indicates the irrigation events for the irrigated treatments F1P3 and F2P3 while the orange arrow indicates the irrigation application for the rainfed plot at the stony soil (F1P2).

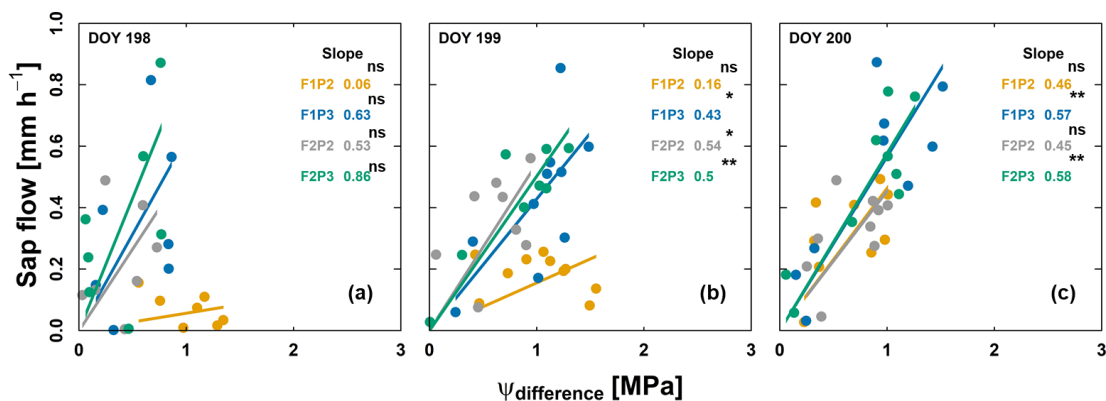


Figure 10: Relationship of sap flow and difference of effective soil water potential and sunlit leaf water potential ($\Psi_{\text{difference}}$) from the rainfed (P2) and irrigated (P3) plots of the stony soil (F1) and silty soil (F2) on three consecutive measurement days from predawn in 2018 (a) DOY 198, (b) DOY 199 and (c) DOY 200. Crop was irrigated on 18 July (DOY 199) at 1 PM, 1 PM, and 4 PM for F1P3, F2P3, and F1P2, respectively (22.75 mm for each plot). The unit of slope in the linear regression (or soil-plant hydraulic conductance) is $\text{mm h}^{-1} \text{MPa}^{-1}$. Regression was based on the DEMING approach. The asterisk which are next to the slopes indicate a significant correlation between two variables according to Pearson method (ns: non-significant; * $p < 0.05$; ** $p < 0.01$; *** $p < 0.001$).

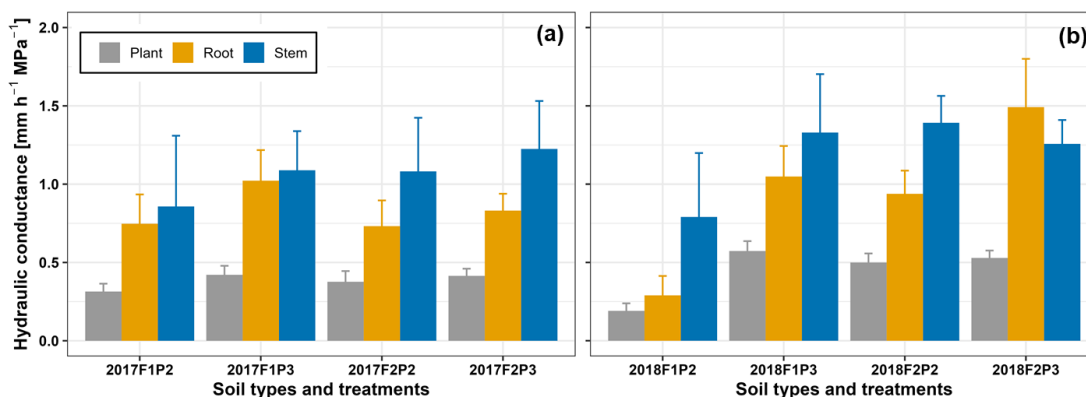


Figure 11: Comparison of different midday hydraulic components ($\text{mm h}^{-1} \text{MPa}^{-1}$): soil-plant (grey bars), soil-root (yellow bars), and stem (blue bars) from the rainfed (P2) and irrigated (P3) plots of the stony soil (F1) and silty soil (F2) in the two growing seasons (a) in 2017 and (b) in 2018. The error bars indicate the standard deviation from measurements around midday (11 AM, 12AM, 1PM, and 2 PM) in different measured days (in 2017 with $n = 4 \times 9$ days, Supplementary material 6, 7, and Fig. 8 and in 2018 with $n = 4 \times 10$ days, Supplementary material 6, 8, and Fig. 9).

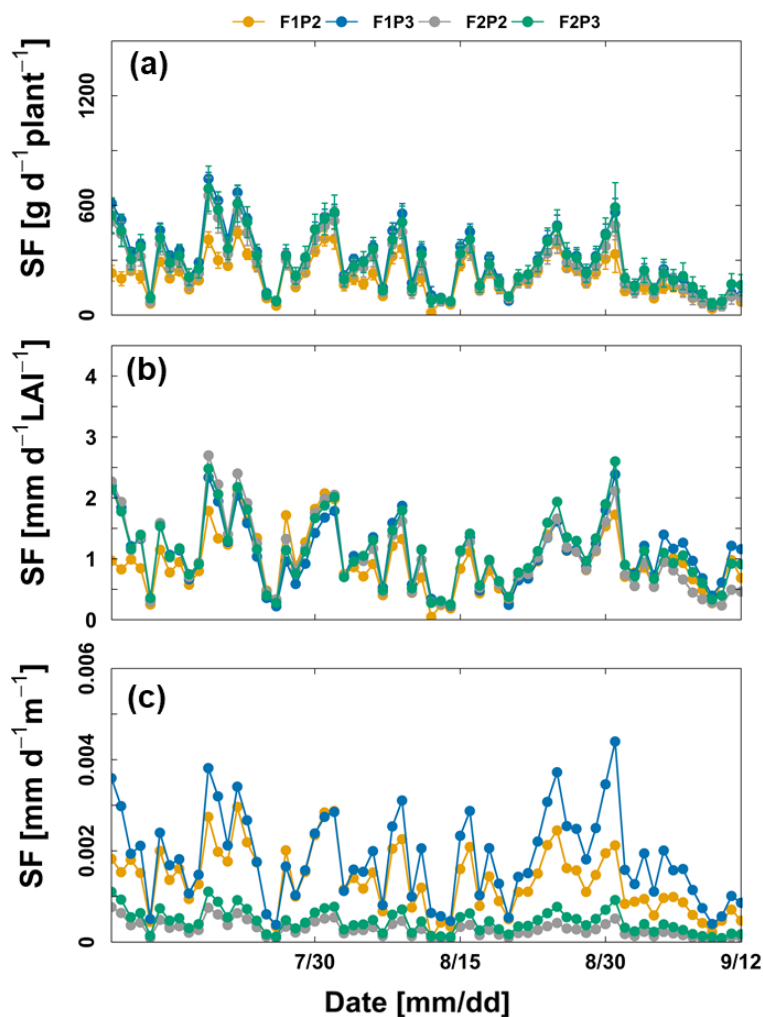


Figure 12: Comparison of sap flow (SF) in growing season 2017 from the rainfed (P2) and irrigated (P3) plots of the stony soil (F1) and silty soil (F2) with (a) sap flow per single plant (b) sap flow per leaf area index (LAI) and (c) sap flow per total root length. Data is shown from 9 July to 12 September 2017. Error bars in (a) indicate the standard deviation of the sap flow measurements in the five different maize plants.

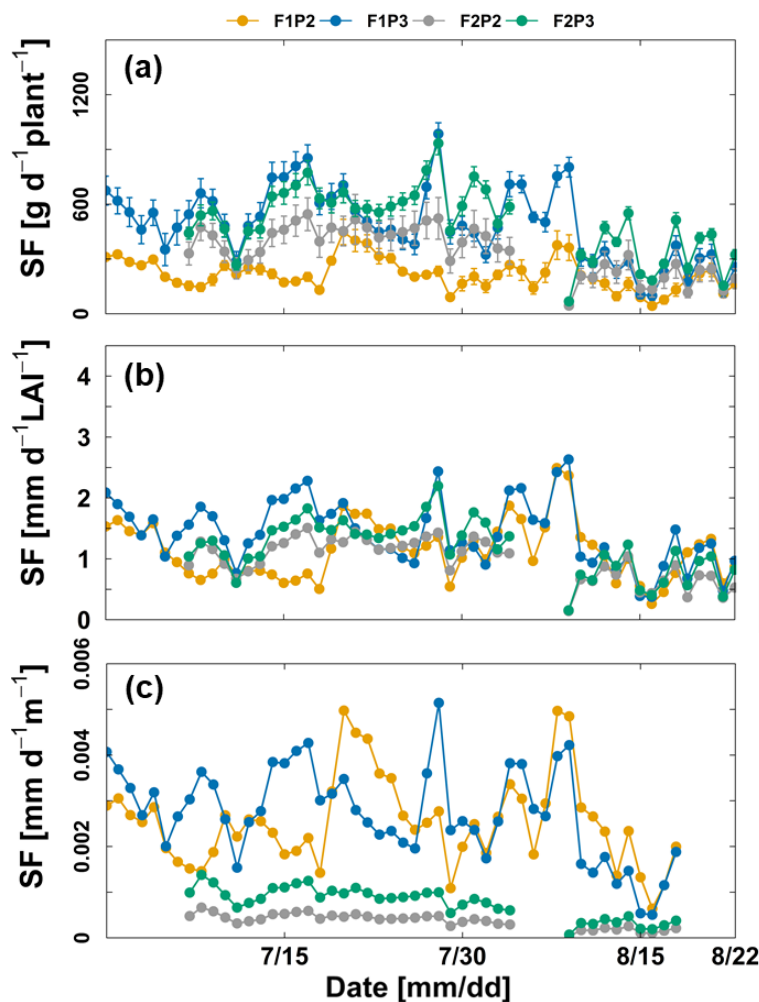


Figure 13: Comparison of sap flow (SF) in growing season 2018 from the rainfed (P2) and irrigated (P3) plots of the stony soil (F1) and silty soil (F2) with (a) sap flow per single plant (b) sap flow per leaf area index (LAI) and (c) sap flow per total root length. Data is shown in (a, b) from 29 June and 6 July for the stony soil (F1) and silty soil (F2), respectively to 21 August, 2018. Missing values of the beginning of the growing season and from 3 August to 6 August 2018 in the F2P2 and F2P3 were due to the missing values of measured sap flow because of sensor disconnection. Missing values in (c) at the end of the growing season in F2P2 and F2P3 was due to no availability of root measurement. Error bars in (a) indicate the standard deviation of the sap flow measurements in the five different maize plants.

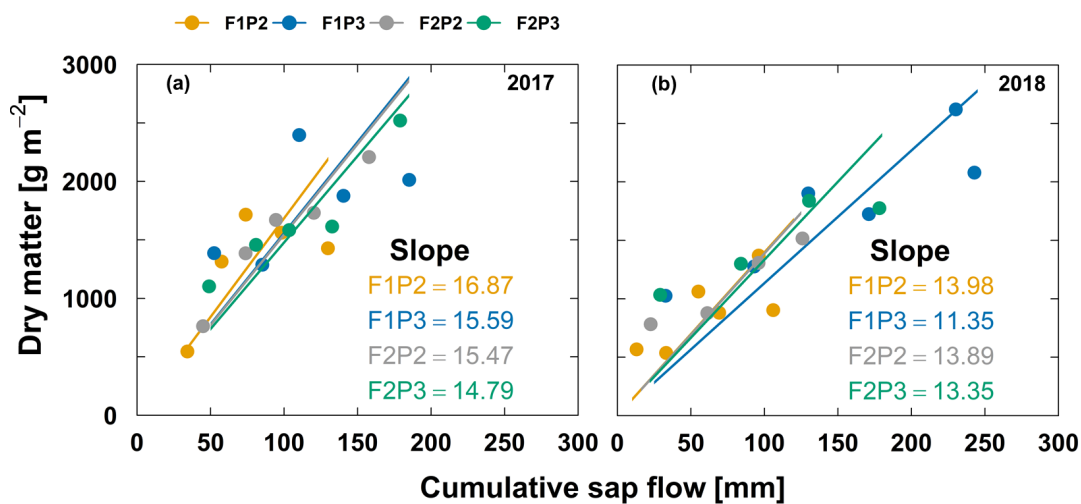


Figure 14: Relationship of aboveground dry matter and cumulative sap flow from the rainfed (P2) and irrigated (P3) plots of the stony soil (F1) and silty soil (F2) in the two growing seasons (a) 2017 and (b) 2018. The unit of slope linear relationship is g mm^{-1} . The less number of data points in (b) in 2018 from the F2P2 and F2P3 plots were due to the missing values of measured sap flow because of sensor disconnection.



1 **Acknowledgements**

2 This work has partially been funded by Federal Ministry of Education and Research (BMBF through
3 European SUSCAP project – 031B0170B). We acknowledge the support by the SFB/TR32 “Pattern in Soil–
4 Vegetation–Atmosphere Systems: Monitoring, Modelling, and Data Assimilation” funded by the Deutsche
5 Forschungsgemeinschaft (DFG). Thuy Nguyen and Thomas Gaiser also thank the DETECT – CRC 1502
6 research program which is funded by DFG. We thank Dr. Matthias Langensiepen for his supports and
7 technical help in the TR32 project. We would like to thank all the student assistants and technicians for
8 their considerable efforts to collect the data in the field and the laboratories.

9

10

11

12

13

14

15

16

17

18

19

20



21 Reference

- 22 Abdalla, M., M.A. Ahmed, G. Cai, F. Wankmüller, N. Schwartz, et al. 2022. Stomatal closure during water
23 deficit is controlled by below-ground hydraulics. *Ann. Bot.* 129(2): 161–170. doi:
24 10.1093/aob/mcab141.
- 25 Abdalla, M., A. Carminati, G. Cai, M. Javaux, and M.A. Ahmed. 2021. Stomatal closure of tomato under
26 drought is driven by an increase in soil-root hydraulic resistance. *Plant. Cell Environ.* 44(2): 425–
27 431. doi: 10.1111/pce.13939.
- 28 Ahmed, M.A., M. Zarebanadkouki, F. Meunier, M. Javaux, A. Kaestner, et al. 2018. Root type matters:
29 Measurement of water uptake by seminal, crown, and lateral roots in maize. *J. Exp. Bot.* 69(5): 1199–
30 1206. doi: 10.1093/jxb/erx439.
- 31 Aparicio-Tejo, P., and J.S. Boyer. 1983. Significance of Accelerated Leaf Senescence at Low Water Potentials
32 for Water Loss and Grain Yield in Maize1. *Crop Sci.* 23(6): crops1983.0011183X002300060040x. doi:
33 <https://doi.org/10.2135/cropsci1983.0011183X002300060040x>.
- 34 Bauer, F.M., L. Lärm, S. Morandage, G. Lobet, J. Vanderborght, et al. 2021. Combining deep learning and
35 automated feature extraction to analyze minirhizotron images: development and validation of a new
36 pipeline. *bioRxiv* (1): 2021.12.01.470811.
37 <https://www.biorxiv.org/content/10.1101/2021.12.01.470811v1%0Ahttps://www.biorxiv.org/content/10.1101/2021.12.01.470811v1.abstract>.
- 39 Bornemann*, L., M. Herbst, G. Welp, H. Vereecken, and W. Amelung. 2011. Rock Fragments Control Size
40 and Saturation of Organic Carbon Pools in Agricultural Topsoil. *Soil Sci. Soc. Am. J.* 75(5): 1898. doi:
41 10.2136/sssaj2010.0454.
- 42 Bourbia, I., C. Pritzkow, and T.J. Brodribb. 2021. Herb and conifer roots show similar high sensitivity to
43 water deficit. *Plant Physiol.* 186(4): 1908–1918. doi: 10.1093/plphys/kiab207.
- 44 Cai, G., M.A. Ahmed, M. Abdalla, and A. Carminati. 2022a. Root hydraulic phenotypes impacting water
45 uptake in drying soils. *Plant Cell Environ.* 45(3): 650–663. doi: 10.1111/pce.14259.
- 46 Cai, G., M. König, A. Carminati, M. Abdalla, M. Javaux, et al. 2022b. Transpiration response to soil drying
47 and vapor pressure deficit is soil texture specific. *Plant Soil* (0123456789). doi: 10.1007/s11104-022-
48 05818-2.
- 49 Cai, G., J. Vanderborght, V. Couvreur, C.M. Mboh, and H. Vereecken. 2017a. Parameterization of Root
50 Water Uptake Models Considering Dynamic Root Distributions and Water Uptake Compensation.
51 *Vadose Zo. J.* 0(0): 0. doi: 10.2136/vzj2016.12.0125.
- 52 Cai, G., J. Vanderborght, A. Klotzsche, J. van der Kruk, J. Neumann, et al. 2016. Construction of
53 Minirhizotron Facilities for Investigating Root Zone Processes. *Vadose Zo. J.* 15(9): 0. doi:
54 10.2136/vzj2016.05.0043.
- 55 Cai, G., J. Vanderborght, M. Langensiepen, A. Schnepf, H. Hüging, et al. 2018. Root growth, water uptake,
56 and sap flow of winter wheat in response to different soil water conditions. *Hydrol. Earth Syst. Sci.*
57 22(4): 2449–2470. doi: 10.5194/hess-22-2449-2018.
- 58 Cai, Q., Y. Zhang, Z. Sun, J. Zheng, W. Bai, et al. 2017b. Morphological plasticity of root growth under mild
59 water stress increases water use efficiency without reducing yield in maize. *Biogeosciences* 14(16):
60 3851–3858. doi: 10.5194/bg-14-3851-2017.



- 61 Carminati, A., and M. Javaux. 2020. Soil Rather Than Xylem Vulnerability Controls Stomatal Response to
62 Drought. *Trends Plant Sci.* 25(9): 868–880. doi: 10.1016/j.tplants.2020.04.003.
- 63 Carminati, A., M. Zarebanadkouki, E. Kroener, M.A. Ahmed, and M. Holz. 2016. Biophysical rhizosphere
64 processes affecting root water uptake. *Ann. Bot.* 118(4): 561–571. doi: 10.1093/aob/mcw113.
- 65 Choudhary, S., and T.R. Sinclair. 2014. Hydraulic conductance differences among sorghum genotypes to
66 explain variation in restricted transpiration rates. *Funct. Plant Biol.* 41(3): 270–275. doi:
67 10.1071/FP13246.
- 68 Cochard, H. 2002. Xylem embolism and drought-induced stomatal closure in maize. *Planta* 215(3): 466–
69 471. doi: 10.1007/s00425-002-0766-9.
- 70 Comas, L.H., S.R. Becker, V.M. V. Cruz, P.F. Byrne, and D.A. Dierig. 2013. Root traits contributing to plant
71 productivity under drought. *Front. Plant Sci.* 4(NOV): 1–16. doi: 10.3389/fpls.2013.00442.
- 72 Coupel-Ledru, A., É. Lebon, A. Christophe, A. Doligez, L. Cabrera-Bosquet, et al. 2014. Genetic variation in
73 a grapevine progeny (*Vitis vinifera* L. cvs GrenachexSyrah) reveals inconsistencies between
74 maintenance of daytime leaf water potential and response of transpiration rate under drought. *J.*
75 *Exp. Bot.* 65(21): 6205–6218. doi: 10.1093/jxb/eru228.
- 76 Couvreur, V., J. Vanderborght, X. Draye, and M. Javaux. 2014. Dynamic aspects of soil water availability for
77 isohydric plants: Focus on root hydraulic resistances. *water Resour. Res.* 50: 8891–8906. doi:
78 10.1002/2014WR015608.Received.
- 79 Couvreur, V., J. Vanderborght, and M. Javaux. 2012. A simple three-dimensional macroscopic root water
80 uptake model based on the hydraulic architecture approach. *Hydrol. Earth Syst. Sci.* 16: 2957–2971.
81 doi: 10.5194/hess-16-2957-2012.
- 82 Daryanto, S., L. Wang, and P. Jacinthe. 2016. Global Synthesis of Drought Effects on Maize and Wheat
83 Production. *PLoS One* 11(5): 1–15. doi: 10.1371/journal.pone.0156362.
- 84 Draye, X., Y. Kim, G. Lobet, and M. Javaux. 2010. Model-assisted integration of physiological and
85 environmental constraints affecting the dynamic and spatial patterns of root water uptake from
86 soils. *J. Exp. Bot.* 61(8): 2145–2155. doi: 10.1093/jxb/erq077.
- 87 Domec, J., and D.M. Johnson. 2012. Does homeostasis or disturbance of homeostasis in minimum leaf
88 water potential explain the isohydric versus anisohydric behavior of *Vitis vinifera* L. cultivars? *Tree*
89 32: 245–248. doi: 10.1093/treephys/tps013.
- 90 Domec, J., and M.L. Pruyne. 2008. Bole girdling affects metabolic properties and root, trunk and branch
91 hydraulics of young ponderosa pine trees. *Tree Physiol.* (28): 1493–1504.
- 92 Dynamax. 2007. Dynagage Sap Flow Sensor User Manual. 1–107. Last access on March 5th 2015.
- 93 Effendi, R., S.B. Priyanto, M. Aqil, and M. Azrai. 2019. Drought adaptation level of maize genotypes based
94 on leaf rolling, temperature, relative moisture content, and grain yield parameters. *IOP Conf. Ser.*
95 *Earth Environ. Sci.* 270(1). doi: 10.1088/1755-1315/270/1/012016.
- 96 Fang, J., and Y. Su. 2019. Effects of Soils and Irrigation Volume on Maize Yield, Irrigation Water Productivity,
97 and Nitrogen Uptake. *Sci. Rep.* 9(1): 1–11. doi: 10.1038/s41598-019-41447-z.
- 98 Frensch, J., and E. Steudle. 1989. Axial and Radial Hydraulic Resistance to Roots of Maize (*Zea mays* L.).
99 *Plant Physiol.* 91: 719–726.



- 100 Gallardo, M., J. Eastham, P.J. Gregory, and N.C. Turner. 1996. A comparison of plant hydraulic
101 conductances in wheat and lupins. *J. Exp. Bot.* 47(295): 233–239. doi: 10.1093/jxb/47.2.233.
- 102 Hochberg, U., F.E. Rockwell, N.M. Holbrook, and H. Cochard. 2018. Iso/Anisohydry: A Plant–Environment
103 Interaction Rather Than a Simple Hydraulic Trait. *Trends Plant Sci.* 23(2): 112–120. doi:
104 10.1016/j.tplants.2017.11.002.
- 105 Hopmans, J.W., and K.L. Bristow. 2002. Current Capabilities and Future Needs of Root Water and
106 Nutrient Uptake Modeling. In: Sparks, D.L.B.T.-A. in A., editor, *Advances in Agronomy*. Academic
107 Press. p. 103–183
- 108 Hubbard, R.M., M.G. Ryan, V. Stiller, and J.S. Sperry. 2001. Stomatal conductance and photosynthesis vary
109 linearly with plant hydraulic conductance in ponderosa pine. *Plant, Cell Environ.* 24(1): 113–121. doi:
110 10.1046/j.1365-3040.2001.00660.x.
- 111 IPCC. 2022. Impacts, Adaptation, and Vulnerability. Working Group II Contribution to the IPCC Sixth
112 Assessment Report of the Intergovernmental Panel on Climate Change.
- 113 Jorda, H., M.A. Ahmed, M. Javaux, A. Carminati, P. Dudgeon, et al. 2022. Field scale plant water relation of
114 maize (*Zea mays*) under drought – impact of root hairs and soil texture. *Plant Soil* 478(1–2): 59–84.
115 doi: 10.1007/s11104-022-05685-x.
- 116 Klein, T. 2014. The variability of stomatal sensitivity to leaf water potential across tree species indicates a
117 continuum between isohydric and anisohydric behaviours. *Funct. Ecol.*: 1313–1320. doi:
118 10.1111/1365-2435.12289.
- 119 Koehler, T., D.S. Moser, Á. Botezatu, T. Murugesan, S. Kaliamoorthy, et al. 2022. Going underground: soil
120 hydraulic properties impacting maize responsiveness to water deficit. *Plant Soil* 478(1–2): 43–58. doi:
121 10.1007/s11104-022-05656-2.
- 122 Li, X., T.R. Sinclair, and L. Bagherzadi. 2016. Hydraulic Conductivity Changes in Soybean Plant-Soil System
123 with Decreasing Soil Volumetric Water Content. *J. Crop Improv.* 30(6): 713–723. doi:
124 10.1080/15427528.2016.1231729.
- 125 Li, Y., J.S. Sperry, and M. Shao. 2009. Hydraulic conductance and vulnerability to cavitation in corn (*Zea*
126 *mays* L.) hybrids of differing drought resistance. *Environ. Exp. Bot.* 66(2): 341–346. doi:
127 10.1016/j.envexpbot.2009.02.001.
- 128 Marin, M., D.S. Feeney, L.K. Brown, M. Naveed, S. Ruiz, et al. 2021. Significance of root hairs for plant
129 performance under contrasting field conditions and water deficit. *Ann. Bot.* 128(1): 1–16. doi:
130 10.1093/aob/mcaa181.
- 131 Meunier, F., A. Heymans, X. Draye, V. Couvreur, M. Javaux, et al. 2020. MARSHAL, a novel tool for virtual
132 phenotyping of maize root system hydraulic architectures. In *Silico Plants* 2(1): 1–15. doi:
133 10.1093/insilicoplants/diz012.
- 134 Meunier, F., M. Zarebanadkouki, M.A. Ahmed, A. Carminati, V. Couvreur, et al. 2018. Hydraulic
135 conductivity of soil-grown lupine and maize unbranched roots and maize root-shoot junctions. *J.*
136 *Plant Physiol.* 227(February): 31–44. doi: 10.1016/j.jplph.2017.12.019.
- 137 Morandage, S., J. Vanderborght, M. Zörner, G. Cai, D. Leitner, et al. 2021. Root architecture development
138 in stony soils. *Vadose Zo. J.* (April): 1–17. doi: 10.1002/vzj2.20133.
- 139 Müllers, Y., J.A. Postma, H. Poorter, and D. van Dusschoten. 2022. Stomatal conductance tracks soil-to-leaf



- 140 hydraulic conductance in faba bean and maize during soil drying. *Plant Physiol.* doi:
141 10.1093/plphys/kiac422.
- 142 Nguyen, T.H., M. Langensiepen, T. Gaiser, H. Webber, H. Ahrends, et al. 2022a. Responses of winter wheat
143 and maize to varying soil moisture: From leaf to canopy. *Agric. For. Meteorol.* 314(December 2021):
144 108803. doi: 10.1016/j.agrformet.2021.108803.
- 145 Nguyen, T.H., M. Langensiepen, H. Hueging, T. Gaiser, S.J. Seidel, et al. 2022b. Expansion and evaluation
146 of two coupled root–shoot models in simulating CO₂ and H₂O fluxes and growth of maize. *Vadose*
147 *Zo. J.* 21(3): 1–31. doi: 10.1002/vzj2.20181.
- 148 Nguyen, T.H., M. Langensiepen, J. Vanderborght, H. Hüging, C.M. Mboh, et al. 2020. Comparison of root
149 water uptake models in simulating CO₂ and H₂O fluxes and growth of wheat. *Hydrol. Earth Syst. Sci.*
150 (24): 4943–4969. doi: 10.5194/hess-24-4943-2020.
- 151 Ordóñez, R.A., S. V. Archontoulis, R. Martinez-Feria, J.L. Hatfield, E.E. Wright, et al. 2020. Root to shoot
152 and carbon to nitrogen ratios of maize and soybean crops in the US Midwest. *Eur. J. Agron.* 120(June):
153 126130. doi: 10.1016/j.eja.2020.126130.
- 154 Passioura, J.B., 2006. The perils of pot experiments. *Funct. Plant Biol.* 33 (12), 1075–1079.
155 <https://doi.org/10.1071/FP06223>.
- 156 Ranawana SRWMCJK, Siddique KHM, Palta JA et al (2021) Stomata coordinate with plant hydraulics to
157 regulate transpiration response to vapour pressure deficit in wheat. *Functional Plant Biol* 48:839–850.
158 <https://doi.org/10.1071/FP20392>
- 159 Richards, R.A., G.J. Rebetzke, A.G. Condon, and A.F. van Herwaarden. 2002. Breeding Opportunities for
160 Increasing the Efficiency of Water Use and Crop Yield in Temperate Cereals. *Crop Sci.* 42(1): 111–
161 121. doi: 10.2135/cropsci2002.1110.
- 162 Rodriguez-Dominguez, C.M., and T.J. Brodribb. 2019. Declining root water transport drives stomatal
163 closure in olive under. *New Phytol.* 225: 126–134.
- 164 Sinclair, T.R., and M.M. Ludlow. 1986. Influence of soil water supply on the plant water balance of four
165 tropical grain legumes. *Aust. J. Plant Physiol.* 13: 329–341.
- 166 Scharwies, J.D., and J.R. Dinneny. 2019. Water transport, perception, and response in plants. *J. Plant Res.*
167 132(3): 311–324. doi: 10.1007/s10265-019-01089-8.
- 168 Schultz, H.R. 2003. Differences in hydraulic architecture account for near-isohydric and anisohydric
169 behaviour of two field-grown *Vitis vinifera* L. cultivars during drought. *Plant, Cell Environ.* 26(8):
170 1393–1405. doi: 10.1046/j.1365-3040.2003.01064.x.
- 171 Stadler, A., S. Rudolph, M. Kupisch, M. Langensiepen, J. van der Kruk, et al. 2015. Quantifying the effects
172 of soil variability on crop growth using apparent soil electrical conductivity measurements. *Eur. J.*
173 *Agron.* 64: 8–20. doi: 10.1016/j.eja.2014.12.004.
- 174 Sulis, M., V. Couvreur, J. Keune, G. Cai, I. Trebs, et al. 2019. Incorporating a root water uptake model based
175 on the hydraulic architecture approach in terrestrial systems simulations. *Agric. For. Meteorol.* 269–
176 270: 28–45. doi: <https://doi.org/10.1016/j.agrformet.2019.01.034>.
- 177 Sunita, C., T.R. Sinclair, C.D. Messina, and M. Cooper. 2014. Hydraulic conductance of maize hybrids
178 differing in transpiration response to vapor pressure deficit. *Crop Sci.* 54(3): 1147–1152. doi:
179 10.2135/cropsci2013.05.0303.



- 180 Tardieu, F., X. Draye, and M. Javaux. 2017. Root Water Uptake and Ideotypes of the Root System: Whole-
181 Plant Controls Matter. *Vadose Zo. J.* 16(9): 0. doi: 10.2136/vzj2017.05.0107.
- 182 Tardieu, F., and T. Simonneau. 1998. Variability among species of stomatal control under fluctuating soil
183 water status and evaporative demand: modelling isohydric and anisohydric behaviours. *J. Exp. Bot.*
184 49(March): 419–432. doi: 10.1093/jxb/49.Special_Issue.419.
- 185 Tardieu, F. 2016. Too many partners in root – shoot signals . Does hydraulics qualify as the only signal
186 that feeds back over time for reliable stomatal. *New Phytol.* 212: 802–804.
- 187 Trillo, N., and R.J. Fernández. 2005. Wheat plant hydraulic properties under prolonged experimental
188 drought: Stronger decline in root-system conductance than in leaf area. *Plant Soil* 277(1–2): 277–
189 284. doi: 10.1007/s11104-005-7493-5.
- 190 Tsuda, M., and M.T. Tyree. 1997. Whole-plant hydraulic resistance and vulnerability segmentation in
191 *Acer saccharinum*. *Tree Physiol.* (17): 351–357.
- 192 Turner, N.C., E.D. Schulze, and T. Gollan. 1984. The responses of stomata and leaf gas exchange to vapour
193 pressure deficits and soil water content - I. Species comparisons at high soil water contents.
194 *Oecologia* 63(3): 338–342. doi: 10.1007/BF00390662.
- 195 Tyree, M.T., E.L. Fiscus, S.D. Wullschleger, and M.A. Dixon. 1986. Detection of Xylem Cavitation in Corn
196 under Field Conditions. *Plant Physiol.* 82(2): 597–599. doi: 10.1104/pp.82.2.597.
- 197 Vadez, V. 2014. Root hydraulics : The forgotten side of roots in drought adaptation. *F. Crop. Res.* 165: 15–
198 24.
- 199 Vadez, V., S. Choudhary, J. Kholová, C.T. Hash, R. Srivastava, et al. 2021. Transpiration efficiency: Insights
200 from comparisons of C4cereal species. *J. Exp. Bot.* 72(14): 5221–5234. doi: 10.1093/jxb/erab251.
- 201 Vanderborght, J., V. Couvreur, F. Meunier, A. Schnepf, H. Vereecken, et al. 2021. From hydraulic root
202 architecture models to macroscopic representations of root hydraulics in soil water flow and land
203 surface models. *Hydrol. Earth Syst. Sci.* 25(9): 4835–4860. doi: 10.5194/hess-25-4835-2021.
- 204 Vanderborght, J., A. Graf, C. Steenpass, B. Scharnagl, N. Prolingheuer, et al. 2010. Within-Field Variability
205 of Bare Soil Evapora Θ on Derived from Eddy Covariance Measurements. *Vadose Zo. J.* 9: 943–954.
206 doi: 10.2136/vzj2009.0159.
- 207 Vereecken, H., A. Schnepf, J.W. Hopmans, M. Javaux, D. Or, et al. 2016. Modeling Soil Processes: Review,
208 Key Challenges, and New Perspectives. *Vadose Zo. J.* 15(5): vzj2015.09.0131. doi:
209 10.2136/vzj2015.09.0131.
- 210 Vetterlein, D., M. Phalempin, E. Lippold, S. Schlüter, S. Schreiter, et al. 2022. Root hairs matter at field
211 scale for maize shoot growth and nutrient uptake, but root trait plasticity is primarily triggered by
212 texture and drought. *Plant Soil* 478(1–2): 119–141. doi: 10.1007/s11104-022-05434-0.
- 213 Vitale, L., P. Di Tommasi, C. Arena, A. Fierro, A. Virzo De Santo, et al. 2007. Effects of water stress on gas
214 exchange of field grown *Zea mays* L. in Southern Italy: An analysis at canopy and leaf level. *Acta*
215 *Physiol. Plant.* 29(4): 317–326. doi: 10.1007/s11738-007-0041-6.
- 216 Wang, N., J. Gao, and S. Zhang. 2017. Overcompensation or limitation to photosynthesis and root hydraulic
217 conductance altered by rehydration in seedlings of sorghum and maize. *Crop J.* 5(4): 337–344. doi:
218 10.1016/j.cj.2017.01.005.
- 219 Welcker, C., W. Sadok, G. Dignat, M. Renault, S. Salvi, et al. 2011. A common genetic determinism for



220 sensitivities to soil water deficit and evaporative demand: Meta-analysis of quantitative trait loci and
221 introgression lines of maize. *Plant Physiol.* 157(2): 718–729. doi: 10.1104/pp.111.176479.

222 Zhuang, J., Y. Jin, and T. Miyazaki. 2001. ESTIMATING WATER RETENTION CHARACTERISTIC FROM SOIL
223 PARTICLE-SIZE DISTRIBUTION USING A NON-SIMILAR MEDIA CONCEPT. *Soil Sci.* 166(5).
224 [https://journals.lww.com/soilsci/Fulltext/2001/05000/ESTIMATING_WATER_RETENTION_CHARACT](https://journals.lww.com/soilsci/Fulltext/2001/05000/ESTIMATING_WATER_RETENTION_CHARACTERISTIC_FROM.2.aspx)
225 [ERISTIC_FROM.2.aspx](https://journals.lww.com/soilsci/Fulltext/2001/05000/ESTIMATING_WATER_RETENTION_CHARACTERISTIC_FROM.2.aspx).

226 Zwieniecki, M.A., P.J. Melcher, C.K. Boyce, L. Sack, and N.M. Holbrook. 2002. Hydraulic architecture of leaf
227 venation in *Laurus nobilis* L. *Plant, Cell Environ.* 25(11): 1445–1450. doi: 10.1046/j.1365-
228 3040.2002.00922.x.

229

230

231

232

233

234

235

236

237

238

239

240

241

242

243



244 **Author contribution**

245 Huu Thuy Nguyen, Thomas Gaiser, Jan Vanderborght, and Frank Ewert: Conceptualization; Huu Thuy
246 Nguyen, and Hubert Hüging: Data curation and data quality check (aboveground measurements); Lena
247 Lärm, Felix Bauer, Anja Klotzsche, Jan Vanderborght, and Andrea Schnepf: data curation and data quality
248 check (belowground measurements); Huu Thuy Nguyen: Formal data analysis and visualization; Thomas
249 Gaiser, Jan Vanderborght, Andrea Schnepf, and Frank Ewert: Funding acquisition & Project administration;
250 Huu Thuy Nguyen: writing – original draft; all authors: review, editing, and finalizing the manuscript.

251 **Competing interests**

252 This manuscript has not been published and is not under consideration for publication in any other journal.
253 All authors agreed and approved the manuscript and its submission to this journal. We declare there is no
254 conflict of interest.

255 **Code/Data availability**

256 The meteorological data were collected from a weather station in Selhausen (Germany) which belongs to
257 the TERENO network of terrestrial observatories. Weather data are freely available from the TERENO data
258 portal (<https://www.tereno.net/ddp/dispatch?searchparams=freetext-Selhausen>, last access:
259 October 2020) (TERENO, 2020). The data which were obtained from the minirhizotron facilities (under-
260 and aboveground) are available from the corresponding author on reasonable requests.

261

262